

NOAA Technical Memorandum NMFS



AUGUST 2002

AN OPERATIONAL MODEL TO EVALUATE ASSESSMENT AND MANAGEMENT PROCEDURES FOR THE NORTH PACIFIC SWORDFISH FISHERY

Marc Labelle

NOAA-TM-NMFS-SWFSC-341

U.S. DEPARTMENT OF COMMERCE
National Oceanic and Atmospheric Administration
National Marine Fisheries Service
Southwest Fisheries Science Center

The National Oceanic and Atmospheric Administration (NOAA), organized in 1970, has evolved into an agency which establishes national policies and manages and conserves our oceanic, coastal, and atmospheric resources. An organizational element within NOAA, the Office of Fisheries is responsible for fisheries policy and the direction of the National Marine Fisheries Service (NMFS).

In addition to its formal publications, the NMFS uses the NOAA Technical Memorandum series to issue informal scientific and technical publications when complete formal review and editorial processing are not appropriate or feasible. Documents within this series, however, reflect sound professional work and may be referenced in the formal scientific and technical literature.

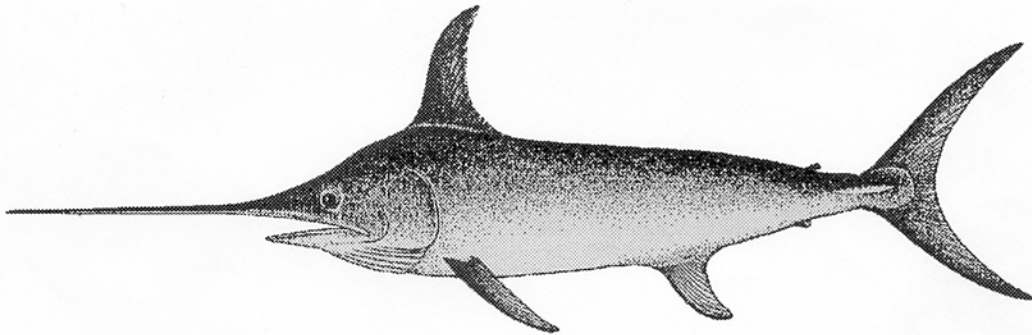


NOAA Technical Memorandum NMFS

This TM series is used for documentation and timely communication of preliminary results, interim reports, or special purpose information. The TMs have not received complete formal review, editorial control, or detailed editing.

AUGUST 2002

AN OPERATIONAL MODEL TO EVALUATE ASSESSMENT AND MANAGEMENT PROCEDURES FOR THE NORTH PACIFIC SWORDFISH FISHERY



Marc Labelle

National Oceanic and Atmospheric Administration
National Marine Fisheries Service
Southwest Fisheries Science Center
2570 Dole Street
Honolulu, Hawaii 96822-2396

NOAA-TM-NMFS-SWFSC-341

U.S. DEPARTMENT OF COMMERCE

Donald L. Evans, Secretary

National Oceanic and Atmospheric Administration

VADM Conrad C. Lautenbacher, Jr., Undersecretary for Oceans and Atmosphere

National Marine Fisheries Service

William T. Hogarth, Assistant Administrator for Fisheries

Abstract

By contrast to several tuna species, relatively little is known about swordfish, and the associated catch and effort statistics are characterized by a substantial level of uncertainty and incompleteness. An operational model was designed to help evaluate the performance of stock assessment and fishery management procedures in this 'data poor' context. This model incorporates key features of age-structured and length-based models and accounts for growth, reproduction, mortality, recruitment, exploitation, and movement. It can be used to project trends in abundance, catch, and stock composition, recruitment patterns, spawning biomass, and so forth, for multiple stocks and fleets, under user-specified levels of process and observation error, sampling regimes, and exploitation patterns. This model has been used to test the performance of stock-assessment procedures and generate preliminary estimates of biological reference points for specific combinations of hypotheses about the fishery. This manuscript describes the features of the model, its underlying hypotheses, limitations, and user interface. The results of probing studies conducted so far are also presented.

1. Introduction

In 1998, the research staff of the Honolulu Laboratory of the National Marine Fisheries Service (NMFS) initiated a project to assess the status of North Pacific swordfish (*Xiphias gladius*). Several agencies in the North Pacific are engaged in stock monitoring and data collection activities aimed at providing information on this species and its fisheries. However, there remains much uncertainty on the demographic traits of this species, the structure and movement patterns of the stock(s), the link between fishing effort and harvest rates, and the stock/fishery interactions.

Given the recognized shortcomings of conventional stock-assessment methods in such contexts, there is a need to design alternative methods that make better use of existing data. This uncertainty also precludes fishery agencies from relying on conventional stock status indicators, so there is also a need to identify alternative reference points for management purposes (see review by Smith et al., 1993; Caddy and Mahon, 1995). To design assessment methods that can make optimal use of deficient data sets and determine the reliability and cost-effectiveness of alternative indicators, one must compare the performance of conventional and new analytical tools using known benchmarks.

In light of the above, plans were made to build a basin-wide simulation model that would mimic key aspects of the population dynamics of swordfish fisheries in the North Pacific, the effects of environmental factors and fleet dynamics, as well as the fishery monitoring and management processes (Kleiber, 1999b). This model could then serve to test the performance and suitability of assessment and management methods under hypothetical but plausible rates of production and exploitation. The effects of measurement and process error, deficiencies in sampling regimes, and survey coverage could be tested for as well. In principle, this approach should lead to the development of powerful analytical tools, increase the reliability of population forecasts, help managers explore the consequences of hypotheses difficult to test empirically, and help formulate scientifically credible fishery management guidelines.

As noted by Hilborn and Walters (1992, p. 239), the use of such 'operational models' (Linhart and Zucchini, 1986) should be an integral part of any stock assessment. Not surprisingly, this approach has been used by NMFS staff in previous swordfish investigations (Goodyear, 1989), by fishery scientists from the Commonwealth Scientific and Industrial Research Organization (CSIRO) to provide better tuna fishery management advice (Campbell et al., 1998), and by stock assessment review committees in Europe (ICES, 1993), and in North America (NRC, 1998).

Work on this model began in April 1998, and a functional version of the model was completed in September 1999. The current version of the model accounts for growth, reproduction, mortality, recruitment, movement, and exploitation of multiple stocks by multiple fisheries over 10 regions. The model can project trends in abundance, catches, recruitment, spawning biomass, and so forth. The overall structure of the current version is given in Appendix I. The following sections provide a description of the main features of this model, including its underlying hypotheses, limitations, user interface, and output capabilities.

2. Model Design

The model is designed to be used by scientists in several agencies. Models that represent single systems or that use nongeneric code preclude porting the code to other compilers or operating systems without making changes and in the process possibly altering the results. Consequently, efforts were made to use a 'platform independent' syntax and user-interface to facilitate portability. The present version is designed to run as a standard console application that interfaces with the user through keyboard input and simple ASCII displays of options and results. The simulation model is written in C++ language so it can easily be linked with sophisticated numerical libraries such as those of IMSL (IMSL, 1989) and AUTODIFF (Fournier, 1992). The model makes minimal use of the standard template libraries (STL; Breymann, 1998) to facilitate portability but does use safe vector and matrices throughout (automatic bounds checking).

Meyers (1997, p. 3) noted that portable code should be developed on at least two compilers to avoid dependence on proprietary language extensions and misapplication of the standard. This model runs on Apple computers with PowerPC processors with OS 9.0 and the Metrowerks C/C++ 5.0 compiler. It also runs on PC computers with Pentium processors with Windows NT and the Visual C++ 6.0 compiler. No part of the code needs to be changed, and the random number sequences are identical on both platforms. The procedure used to link the AUTODIFF libraries to Visual C++ IDE is provided by Otter Research. The procedure to link this library to the Metrowerks IDE is identical to that for linking with other libraries, and needs no further explanation.

During the model development process, efforts were made to use existing models and functions wherever possible since they are documented, understood, and can be referenced. When too little information was available to justify the use of a particular model or function, one was formulated on an ad hoc basis from ecological theory. With the acquisition of new data and additional insight on the fishery, these generic models can be substituted by more appropriate ones.

Efforts were made to structure the model according to the 'state-space' principles described by Schnute (1994). This involves specifying distinct vectors for population attributes, observations, controls, and time-independent parameter values. This framework is suited for the development of sequential fisheries models, can be used for simulation and estimation, can accommodate Bayesian and frequentist views, can help delineate the data limits, and establish rational priorities for future data collection. This framework was used to conduct exploratory analyses elsewhere (Schnute and Richards, 1995; Richards et al., 1997) and is a logical framework to adopt in the present context.

The latest version of the model is not primarily designed to estimate stock or fishery parameters as such. Rather, its main use is in generating time series of observations of certain aspects of the fishery given a set of input parameter values for the various model components (Table 1). Data can be generated with variable resolution and realistic error levels. Sampling periodicity and intensity can be adjusted to conduct sensitivity analyses and help determine the cost:benefit ratios of proposed monitoring programs. The level of bias and noise can be adjusted to

assess the effects of data contamination and measurement errors. The latest version of the model does not account for the influence of oceanographic conditions on all key aspects of population and fishery dynamics, does not make use of priors on process parameters, does not account for all major sources of uncertainty, and does not enable risk analyses to be conducted automatically during each run. In time, the model may be modified to do so if need be.

Once the user has supplied the initial input, the program generates matrices of expected proportions in length-at-age and weight-at-length given the hypothesized growth patterns based on empirical observations. These proportions serve to update the length and weight distributions of the catch and the survivors at given periods. The model then builds the population size through constant recruitment, growth, and natural mortality in one-month time steps. Once the population stabilizes, and the matrix of survivors-at-age is full, the actual simulation begins by implementing various deterministic and stochastic processes. This includes spawning, linking it to recruitment, allowing for movement, accounting for natural and fishing mortality, and conducting sampling and monitoring activities. The bookkeeping process is similar to that of a forward cohort analysis, with several vectors or matrices updated at each one-month time step. These include the numbers alive and caught by sex/age, sex/length, and sex/weight categories. The matrix values maintain a 'snapshot' of the stock state at any time from which other computations are made to provide time series of states, observations, and reference points.

3. Model Notation

i	= subscript denoting a 1cm eye-fork length category (range: 20-300, $I=\max.$)
j	= subscript denoting an age group (range: 1-30, $J=\max.$)
w	= subscript denoting a 1 kg weight category (range: 0-800, $W=\max.$)
s	= subscript denoting sex category (male = 0, female = 1)
y	= subscript denoting the year (range: 0 - ∞)
t	= subscript denoting the month of the year (range: 0-12)
v	= subscript denoting the vessel category (range: 1-4, $V=\max.$)
o	= subscript denoting a region of origin
d	= subscript denoting a region of destination
x_i	= mid-point on the 1 cm length interval if the i th category
P_{ij}	= probability of age j fish being of length i
P_{iw}	= probability of weight w fish being of length i
μ_j	= mean eye-fork length distribution of age j fish (cm)
σ_j	= standard deviation in eye-fork length distribution of age j fish
m	= number of months after birth (range: 0-12)
k	= von Bertalanffy (VB) parameter for maximum growth rate per year
ρ	= Brody growth coefficient (e^{-k})
L_1	= mean eye-fork length of first age group on the VB curve in month 1
L_J	= mean length (EFL) of last age group on the VB curve in month 1
N	= number of fish
k_n	= scaling factors for egg production ($n=1$) and recruitment levels ($n=2$)
M	= natural mortality rate
f	= standardized fishing effort
F	= fishing mortality rate
F'	= effective fishing mortality rate
F^*	= realized fishing mortality rate
Z	= total mortality rate
C	= catch
q	= catchability coefficient
H	= catch reporting rate
S	= selectivity index
E	= egg production
R	= number of recruits
V	= fish movement rate due to swimming and current velocities ($\text{km}\cdot\text{d}^{-1}$)
W	= width between opposite boundaries in direction of travel (km)
B	= boundary length (in km)
Γ_i	= proportion length in fish that are mature
η	= effective spawners
η^*	= equilibrium level of effective spawners
λ	= mating success probability (range: 0-1)
ϕ_i	= fecundity of length in female
ε	= random deviate from $N(0;\sigma^2)$
ω	= residual deviation
γ	= non-linearity coefficient (=1.0 unless specified otherwise)
θ	= sea surface temperature score
∇	= sea surface temperature gradient index
u_{od}	= displacement rate across a region of origin and destination ($\%N\cdot\text{d}^{-1}$)
a_n, b_n	= generic model coefficients ($n = 0$)

4. Biological Components

4.1 Growth Patterns

4.1.1 Length-at-age

Numerous studies have reported dimorphic growth in swordfish, with females attaining larger mean size-at-age than males. Swordfish growth conforms well to the von Bertalanffy model, so the latter is used to predict the mean length-at-age and the age group contributions to each size category. Examination of the length/age data provided by E. DeMartini (pers. comm.) and Uchiyama et al. (1999) suggested these were adequate to provide estimates of the von Bertalanffy parameters and mean length-at-age (Fig. 1) but insufficient to determine variation in length-at-age with certainty. For several species, including tuna, this variation is thought to be a function of mean length-at-age (Fournier et al., 1990; Labelle et al., 1993). Further examination of the length/age data revealed a curvilinear relation between these variables for both sexes, with the maximum variation at eye-to-fork length (EFL) of about 140 cm (Fig. 2).

A quadratic function was found to be adequate for predicting standard deviations from the means. The function fitted the data well for both sexes ($r^2 = 0.69$ and 0.56 , respectively) over all age groups with at least six age-length observations, and no aberrant pattern was detected in the residuals for males and females. The von Bertalanffy and quadratic models were used to compute the probability of swordfish of a given age and sex being in a length interval. The re-parameterized version of the von Bertalanffy model proposed by Schnute and Fournier (1980) is used to compute by probabilities using sex-specific estimates of parameters L_1 , L_J , K , b_0 , b_1 and b_2

$$(4.1.1) \quad s_j = b_0 + b_1 u_j + b_2 u_j^2 .$$

$$(4.1.2) \quad m_j = L_1 + (L_J - L_1) \left\{ \frac{1 - r^{j-1+(m/12)}}{1 - r^{J-1}} \right\} .$$

$$(4.1.3) \quad P_{ij}(u_j, s_j) = \frac{1}{\sqrt{2\pi s_j}} \exp \left\{ -\frac{(x_i - u_j)^2}{2s_j^2} \right\} .$$

Probabilities are computed for the 20-300 cm size range, by 2-cm size intervals (20.00-21.99 cm = 21 cm category = index 1). For convenience, L_1 corresponds to length at age-1, or the size at which swordfish show up in longline catches in substantial numbers. The parameter values used are $L_1=90.81$, $L_J=227.10$, $K=0.17$, $b_0=-25.74$, $b_1=0.70$ and $b_2=-0.0026$ for males, and $L_1=95.85$, $L_J=273.4$, $K=0.14$, $b_0=-23.6$, $b_1=0.636$ and $b_2=-0.002$ for females. The predicted growth trends indicate that females grow faster than males, and reach L_∞ at about 30 years of age.

4.1.2 Weight-at-length

Commercially caught swordfish are typically dressed (bill, head, and entails removed) before being landed at markets, so the most commonly reported weight is

for this category of fish. Uchiyama et al. (1999) noted that the relation between dressed weight and eye-fork length conformed to a power function of the type $W = aL^b$. The authors found that sex and season had a statistically significant effect on the relation observed for swordfish caught by the commercial fishery in Hawaii during 1994-96. The average weight for males was slightly heavier than females of the same length, and weights tended to be greater during the first half of the calendar year before the spawning season. In general, condition was more strongly influenced by month than by sex.

Swordfish gonads are generally removed long before weighing, so commercial weight records can rarely be separated by sex category. A single weight-length relation is thus used to predict the dressed weights of males and females within a month, but separate relations are used to predict mean weight-at-length each month. The parameter estimates reported by Uchiyama et al. (1999) were used for this purpose, except for September and December that were substituted by those of October and January, which were based on larger sample sizes.

Examination of the corresponding weight and length measurements collected during 1994-96 indicated that a linear relation (without an intercept) existed between the standard deviation and the mean weight-at-length over the 24-200 cm size range. The slope coefficient was estimated to be 0.133, and the relation fitted the data well over this range ($r^2=0.99$). The probability of a length i fish being in a given weight category was predicted by modifying the indices of Eq. 4.1.3, and substituting Eq. 4.1.1-4.1.2 such that the mean and variance in weight-at-length were predicted from the power and linear functions described above. Probabilities were computed for the 0-800 kg range, by two kg intervals (0-1.99 kg=1 kg category=index 1).

4.1.3 Length-at-weight

The probability of a weight k fish being of length i was determined from the data (sexes combined) reported by Uchiyama et al. (1999). Examination of the relation between the standard deviation and mean length by 20 kg weight categories indicated that the standard deviations increased linearly to about 210 cm EFL (or 135 kg) and decreased to zero as size progresses towards L_∞ . A breakpoint regression (Neter et al., 1985) was used to predict the standard deviations from the means. A regression of the form $Y=a+b_0X$ was used to predict values below the breakpoint, and a second regression $Y=a+b_0X+b_1(X-\text{breakpoint})$ was used to predict values above it. Parameters a , b_0 , b_1 , and the breakpoint were estimated to be -0.694391, 0.044533, -0.190743, and 208.7806, respectively. The predicted values match the observed ones fairly well (Fig. 3, $r^2=0.72$). After making the substitutions described previously, the probabilities were computed for the 0-800 kg range, by 2-kg intervals (0-1.99 kg=1 kg category=index 1).

4.2 Depletion

The number of fish surviving exploitation is a function of previous abundance, natural mortality, and fishing mortality. The latter two processes are modeled as instantaneous rates to use the conventional form of the catch equation. Typically, not all size groups are equally susceptible to capture by a gear type, so the model uses size selectivity curves to compute catch by gear (or vessel) type. Size selectivity is

modeled as a fixed gear (vessel) effect, distinct from catchability that is considered to be a variable, time-independent, gear effect. The model converts numbers-at-age to numbers-at-length, that are subject to size-specific F . The survivors-at-length and catch-at-length are then converted back to catch-at-age and survivors-at-age. Different gear (or vessel) types can harvest the same stock in a stratum, so the model accounts for combined impacts.

$$(4.2.1) \quad F_{vt} = q_v f_{vt}^g e^{e-0.5s_{qv}^2} .$$

$$(4.2.2) \quad F'_{it} = \sum_{v=1}^V F_{vt} S_{iv} .$$

$$(4.2.3) \quad Z_{ijt} = F'_{it} + M_{jt} .$$

$$(4.2.4) \quad N_{j,t+1} = \sum_{i=1}^I N_{ijt} e^{-Z_{ijt}} .$$

$$(4.2.5) \quad C_{ijt} = \frac{F'_{it}}{Z_{ijt}} (1 - e^{-Z_{ijt}}) N_{ijt} .$$

$$(4.2.6) \quad C_{ijvt} = \frac{F_{vt} S_{iv} C_{ijt}}{F'_{it}} .$$

$$(4.2.7) \quad F_{jt}^* = -\ln \left(\frac{N_{j+1,t+1}}{N_{jt}} \right) - M_{jt} .$$

Total catch by length and age categories are dissociated into catch by vessel type based on the contribution of the fleet to the total effective fishing mortality. In the absence of information on gear selectivity for North Pacific fisheries by time and area, two patterns were used in the present study. For Pacific longline fisheries, Hinton and Deriso (1998) assumed that knife-edge recruitment of swordfish occurred at about 100 cm (eye-fork length). By contrast, Kimura and Scott (1994), and Prager et al. (1996) used a logistic relation to predict the overall selectivity for swordfish (from lower jaw-fork length, LJFL) harvested by a combination of longline, harpoon, drift gillnet, and recreational fisheries in the Atlantic.

The relation between eye-fork lengths (EF) and lower jaw-fork lengths of Pacific and Atlantic populations were assumed to be similar and to conform to that described by DeMartini et al. (in prep.) for the North Pacific population (LJFL=8.01 + 1.07 EF, $n=179$, $r^2=0.99$). After substituting the LJFL measurements with the EF equivalents, selectivity trends were computed with the coefficients reported by Prager et al. (1996). This curve was used to describe the overall selectivity of a combination of gillnet, harpoon, and recreational fisheries (see later section). For purposes of simplification, a logistic curve was also used to describe the selectivity of longline fisheries, with the parameters chosen such that fish over 100 cm in EFL are fully recruited (Fig. 4). In future versions of the model, additional vessel categories and selectivity curves will be added, and if need be, the selectivity parameter can be allowed to change over time (see NRC 1998, p. 55).

4.3 Reproduction

Reproductive success is modeled as a function of maturation rates, fecundity-at-size, spawning frequency, and spawning biomass. To ensure biological realism, spawning success should decline when biomass drops below some threshold value, such that the population can collapse under sustained and excessive exploitation. This is akin to allowing for Allee effects (see Allee et al., 1949), where per capita growth rates decrease at low densities. Under such conditions, there is an increasing probability that potential mates cannot find each other, thus reducing mating success.

4.3.1 Maturation

DeMartini et al. (in prep.) predicted the proportion at maturity of males and females with the logistic model using the EFL interval as the independent variable (Eq. 4.3.1). They reported estimates of parameters a and b of 14.401 and 0.141 respectively for males, and 14.857 and 0.103 for females. The predicted proportions, and the corresponding number of fish alive, are used to compute the number of 'effective spawners' which serves as an index of spawning intensity

$$(4.3.1) \quad \Gamma_{si} = \frac{1}{1 + e^{a-bi}} .$$

$$(4.3.2) \quad h_{st} = \sum_{i=1}^I \Gamma_{si} N_{ist} .$$

4.3.2 Mating success

Not all gravid females are necessarily fertilized during each spawning period. Densities may be too low for potential mates to contact, or the sex ratios may be so unbalanced that too few males are available. A model based on Holling's (1959) disk equation is used to predict mating success (see Appendix II for derivations). For a given stratum, the probability of successfully mating is predicted from the relative number of effective spawners and the availability of males

$$(4.3.3) \quad t = 100 \frac{h_1 + h_0}{h_0^* + h_1^*} .$$

$$(4.3.4) \quad p = \frac{e^{a+bt}}{1 + e^{a+bt}} .$$

$$(4.3.5) \quad l = \frac{\frac{h_0}{h_1} ph}{1 + \left(\frac{h_0}{h_1} ph \right)} .$$

Values for parameters a , b , and h can be selected arbitrarily to make the predicted trend conform to some plausible pattern. The values selected were -7, 1.3, and 100 respectively, so the probability of contact is about 1.0 when the number of effective spawners is =10% of the equilibrium level, and declines in a sigmoid

fashion to zero below this level (Fig. 5). As a result, reduced spawning success is obtained only under low abundance levels and reduced male availability (Fig. 6).

4.3.3 Egg production

Uchiyama and Shomura (1974) hypothesized that swordfish spawned near Hawaii from April through July, and noted that fecundity increases with body weight, with 200-kg females being about twice as fecund as those weighing 80 kg. Recent surveys found swordfish larvae near Hawaii during April-September and small juveniles of 19 cm EFL during October (R. Humphreys, pers. comm.). It is thus hypothesized that swordfish spawn during March-September south of 27°N in the central Pacific (DeMartini et al., in prep.) and south of 30°N west of 160°E (Graal et al., 1983, Nishikawa et al., 1985) because warmer surface waters extend further north in that area. No spawning activity is thought to occur east of 120°W.

Arocha and Lee (1995) noted that Atlantic swordfish spawned during December to February in waters at 19-23°N, and in coastal waters at 24-34°N and oceanic waters at 13-17°N during March-June. On average, females spawned every 3 d during this period, but no data are available on the link between body size and spawning frequency. Arocha (1997) found that the relation between batch fecundity and lower jaw-fork length (L, in cm) conformed to the power function of the form $Y=a+bL^c$, with parameters a, b, and c being 1757430, 11.575 and 2.8814, respectively. Assuming the relation between eye-fork lengths (i) and lower jaw-fork lengths is identical for the Pacific and Atlantic stocks and conforms to that described by DeMartini et al. (in prep.) for the Pacific stock ($L = 8.01+1.07i$, $n=179$, $r^2=0.992$), an egg production index is computed from

$$(4.3.6) \quad f_i = 1757430 + 11.575(8.01 + 1.07i)^{2.8814} .$$

$$(4.3.7) \quad E_t = I_t \sum_{i=1}^I h_{lit} f_i .$$

4.4 Recruitment

Initially, the model builds up a population by adding 2000 recruits each year. The male:female ratio is assumed to be 1:1, and half of the recruits are added to the age-1 group of each sex category on January 1. After several generations, the unexploited population reaches a steady state. Subsequent recruitment is a function of total egg production from spawning events assumed to occur from March to September. Surviving juveniles recruit to the population at age-1, with age updated on January 1. Consequently, some juveniles enter the age-1 group after < 4 months of growth.

A stock-recruitment function is used to link recruitment to egg production. In the absence of data on Pacific swordfish, assessments of the Atlantic population were used to set the shape of this function. In a simulation model of Atlantic swordfish population dynamics, Prager et al. (1996) hypothesized the existence of a Ricker (1954) stock-recruitment relation. Using estimates from virtual population analyses conducted at ICCAT, Garcia-Saez (1996) detected a significant, non-linear, dome-shaped relation between egg production and recruitment of age-1 fish in

Atlantic swordfish. The data presented by Garcia-Saez (1996) were fitted to two stock-recruit relations, by minimizing the sum of squared deviations.

$$(4.4.1) \quad R = Ee^{a-bE+w} . \quad (\text{Ricker 1954})$$

$$(4.4.2) \quad R = \frac{aEe^w}{b + E} . \quad (\text{Beverton-Holt 1957})$$

Before fitting the model, egg production and recruitment were scaled by 1E-12 and 1E-3 mainly to get productivity-per-spawner estimates in the 0-3 range for purposes of convenience. For the Ricker model, the estimates of parameters a , b , and w were 2.54696, 0.00827, and 0.0231. For the Beverton-Holt model, the parameter estimates were 855.48023, 70.32099, and 0.0471. The Ricker model fit indicates considerably lower productivity per spawner at low stock sizes (Fig. 7) and is more conservative in this regard. Estimates of the replacement levels ($E_r = R_r$) were also computed using the formulae described by Ricker (1975, Appendix III). The estimates obtained for the Ricker and Beverton-Holt models were 307.9 and 785.2, respectively. The stock-recruitment models used in this version do not yet account for possible autocorrelations in the terms, nor do they allow for environmental effects.

The above parameters serve to predict recruitment given the productivity level of the Atlantic population. The objective here is to use a relation of the same shape to predict recruitment in the North Pacific population that may be of different size. This is accomplished by using a scaling factor that relates equilibrium egg production to the estimated replacement levels ($k_1 = E_r/E_{eq}$) and equilibrium recruitment to replacement levels ($k_2 = 2000/R_r$). By applying the scaling factors, one simply matches the relative productivity of the two populations.

The model interface allows the user to specify which model is used to predict recruitment and the magnitude of the error term (ω). Based on the variance of the residuals, this term was set to 0.25 for the simulations discussed in later sections. This value is slightly higher than the residual variance obtained when fitting the models and allowed recruitment to vary by $\pm 30\%$ about the mean. For the Ricker model, recruitment is then predicted from

$$(4.4.3) \quad E_y^* = k_1 \sum_{t=3}^9 E_{yt} .$$

$$(4.4.4) \quad R_{y+1} = k_2 E_y^* e^{a-bE_y^*+e} .$$

The model can predict biomass time series (Fig. 8) that exhibit variation similar to that of natural fish stocks (see examples in Hilborn and Walters, 1992). Trends in abundance predicted with both stock-recruit functions are similar when exploitation rates are low. However, the Beverton-Holt model allows for high productivity at very low stock sizes, so the population is capable of withstanding much higher rates of total mortality without collapsing.

4.5 Stock and Catch Compositions

Three pairs of matrices are updated during the iterations to account for growth, recruitment, and depletion. These are the numbers alive and caught by sex/age and sex/length and sex/weight categories. A direct conversion of numbers-at-age into numbers-at-length is done using the proportions in length-at-age computed at mid-month ($m=0.5, 1.5, \dots, 11.5$). A conversion of numbers-at-length into numbers-at-weight is then conducted using the proportions in weight-at-length

$$(4.5.1) \quad N_{it} = \sum_{j=1}^J N_{jt} P_{ij} .$$

$$(4.5.2) \quad N_{wt} = \sum_{i=1}^I N_{it} P_{iw} .$$

4.6 Natural Mortality

Natural mortality rates of swordfish in the Pacific have not yet been estimated from analysis of tagging data. For assessments of Atlantic swordfish, Prager et al. (1996) hypothesized that M was on the order of $0.1 \cdot \text{yr}^{-1}$ for all age classes of each sex. For Pacific swordfish, numerical simulations suggested that M is on the order of $0.2 \cdot \text{yr}^{-1}$ (P. Kleiber, pers. comm.). Natural mortality rates of swordfish populations in other oceans were also estimated indirectly through various analyses and generally tended to be around 0.2-0.4 (Skillman, 1998). Based on the figures reported by Boggs (1989), Hinton and Deriso (1998) considered 0.6-0.8 to be a reasonable range.

If both sexes are subject to the same growth and mortality rates and exhibit the same distribution and behavior towards longline gear, one would expect comparable contributions to longline catches. However, Demartini and Boggs (1999) observed that the contribution of females to longline catches was about 50% for fish below 150 cm, but increased almost linearly thereafter to reach 100% when fish attained 240 cm. Not enough information is available to determine if the behavior and distribution of males and females differ substantially. However, females grow faster than males and show slightly greater variation in length at younger ages (section 3.1).

Differential mortality has been reported in other species, with higher rates associated with the energetic requirements of gonad production and spawning activity. To assess the effects of differential growth and mortality, exploratory simulations were conducted using the present model. The population was allowed to build up to the 'equilibrium' state, at which time fishing effort was applied, and the contribution of females to longline catches was determined by size category. The simulation was first conducted using the same natural mortality rate ($M=0.2 \cdot \text{yr}^{-1}$) for all age groups of both sexes. The same fishing mortality ($F=0.03 \cdot \text{yr}^{-1}$) was applied to all fish but given the longline size selectivity, not all size categories were subject to the same mortality rate. In the second simulation, the mortality rate for males was increased up to 4 times the rate acting on females ($0.2 = M_{\text{male}} = 0.8$). The initial size at which this higher mortality rate was applied was also allowed to vary, from 50 cm to 160 cm. A simple grid-search procedure (Hilborn and Walters 1992) was done to

find the combination of values that yielded the least-squares fit between the predicted and observed contributions reported by DeMartini and Boggs (1999).

Initial simulations revealed that sex-specific growth patterns are not sufficient to cause an increase in female contributions to longline catches of large swordfish (Fig. 9). The predicted contribution decreases from about 50% to 42% as size increases from 60 to 120 cm. Females are depleted faster than males because of their faster growth and greater size variation. This causes a progressive reduction in the relative abundance of females, at least in the first year of life. The female contribution then stabilizes, and increases only when the female size exceeds the maximum sizes attained by males ($L_{\infty} = 227$ cm).

By contrast, allowing for differential mortality results in a close match between the predicted and observed contributions. The best fit was obtained when M_{male} was 2.34 times greater than that of females and the threshold size was 135 cm, which corresponds to the size at which 100% of the males are mature (DeMartini and Boggs 1999). So when females are subject to $M = 0.2 \cdot \text{yr}^{-1}$, mature males would be subject to $M = 0.476 \cdot \text{yr}^{-1}$, which translates into annual survival rates of about 82% and 62% respectively. Further simulations indicated that the difference between the two rates was a function of the baseline rate applied to females. For female rates of 0.1 and 0.15, the M of males was 0.398 and 0.432 respectively. All three combinations fitted the data almost equally well.

In the absence of evidence to support the existence of other processes accounting for this trend, it is hypothesized that mature males are subject to higher mortality rates than females. Males reach maturity after age-1, while females reach it at around age-3. Perhaps males spend considerable energy seeking and competing for larger females, which in turn makes them more susceptible to dying from various causes. Given the above considerations, differential mortality was used for baseline simulations with $M_{\text{female}} = 0.15$ and $M_{\text{male}} = 0.43$. These values are within the range reported by Skillman (1998) and slightly lower than those hypothesized by Hinton and Deriso (1998).

5. Observation Model

In addition to computing expected results under the basic model, predictions can be made using alternative functions to assess the effects of model misspecification, measurement error, and monitoring deficiencies. Pseudo-observations of catch, age, length, and weight frequencies can be generated, corresponding to actual values contaminated with a user-specified level of bias, error, and stochasticity for various processes.

5.1 Fishing mortality

The relation between fishing effort and fishing mortality (F) expressed in Eq. 2.1 allows the user to investigate hypotheses where fishing mortality is proportional to effort ($\gamma=1$), increases faster than effort ($\gamma>1$), or vice-versa ($\gamma<1$). Stochastic variation in catchability is allowed between fishing incidents, but the user can also change the annual catchability to assess the effects of increased experience and increased fishing efficiency caused by technological advances. The model can thus

provide insight into cases where CPUE is indicative of abundance ($\sigma_q=0.1$, $\gamma=1$), unrelated to it ($\sigma_q=0.5$, $\gamma=0.4$), declines more slowly than abundance, or vice versa. Hilborn and Walters (1992, p. 176) respectively termed the latter two scenarios hyperstability and hyperdepletion.

5.2 Catch observations

Catch statistics generated by the simulator can account for hypothesized misreporting and a mix of measurement, counting, interpretation, and coding errors that can occur prior to data analysis. The model generates catch records from

$$(5.2.1) \quad C_t^{obs} = (H + \mathbf{e}_1)C_t^{act}e^{\mathbf{e}_2-0.5}.$$

The above formulation allows bias and error to be added to the catch associated with each fishing incident. Biased catches are obtained by specifying a reporting rate that differs from 1.0, to which is added normally distributed noise ranging within user-specified bounds. Biased rates of less than 1.0 occur when commercial fishermen do not report discards, or retain more fish than permitted but fail to say so. Biased rates exceeding 1.0 occur when fishermen report more fish than caught, which happens when fishermen misidentify the species caught (C. Boggs, pers. comm.). Noise is added because the reporting rate rarely remains constant across fishing incidents. The noise can be constrained to reflect the suspected variation in reporting rate. For the simulations conducted so far, a unit normal random deviate constrained to $\pm 20\%$ of the mean reporting rate was used as noise. By contrast, the error added to the catch is an unconstrained unit normal random deviate, which allows large deviations from the actual values that would appear as anomalies during subsequent analysis (huge catch, little effort).

5.3 Length observations

Observations taken by the author while on a cruise on the NOAA ship *Townsend Cromwell* during October 1998 revealed that errors made while measuring the eye-fork length of swordfish tend to be negligible. Furthermore, many fishery agencies do not routinely conduct swordfish length sampling operations on board their commercial fleets to obtain representative samples by time/area stratum. (P. Kleiber, pers. comm.). Samples of length frequencies typically stem from observer programs, research and training cruises, port sampling operations, or are occasionally predicted from the weights (whole, dressed, round, loins, and so forth) as reported in commercial logbooks, landing or sale records. Observations conducted by NMFS staff at Honolulu markets indicate that weight measurement errors from the Hawaiian longline fleet landings tend to be negligible due to price considerations (J. Uchiyama, pers. comm.). These facts suggest that the reliability of length-based assessments could be affected by deficiencies in sample coverage or when using samples based on converted weights that are raised (multiplied by reciprocal of sampling rate) to represent all fleet catches during the season. The model can be used to generate pseudo-length observations to investigate this issue.

A direct conversion of weight to length can introduce two types of error. Since the sex of a dressed swordfish is rarely recorded, one can obtain biased estimates of mean length by sex when using the weight-length relation for both sexes combined.

The second error is due to the variance in weight-at-length. Not all fish of a given weight are exactly the same length, so matrices of weight-at-length probabilities are needed to best reconstruct the length-frequency distributions from weight data (for example, see Labelle et al., 1997). When such matrices are unavailable, direct conversions of weights would not account for variation in length at weight.

The simulation model generates pseudo-observations of catch length-frequencies through a combination of two successive processes, namely (i) random sampling from the actual weight frequency distribution of live swordfish in a time/area strata and (ii) a direct conversion of the weights to length. The transformation method described by Press et al. (1992, p. 201) is used to generate random samples. The predicted weight-frequency distribution of the catch is used to construct an empirical probability distribution of weights by dividing each frequency by the sum of frequencies for that time/area stratum. The corresponding cumulative probability distribution forms the definite-integral curve. A uniform deviate (0-1) is then generated, and the corresponding weight on the definite-integral curve is taken as the random weight measurement. This weight is then converted directly to a pseudo-length using the equations reported by Uchiyama et al. (1999) to predict eye-fork length from dressed weight for each month of the year (sexes combined). This process is repeated until the total weight of the samples taken matches the total weight of the catch in the stratum.

5.4 Ageing errors

Ageing errors can translate into biased estimates of growth rates, length at age, catch composition, and year class progression resulting in an assessment failure. The simulator can be used to determine the relative importance of ageing errors on swordfish stock assessment results. The von Bertalanffy growth parameters used in the model are obtained from studies currently underway at the Honolulu Laboratory. NMFS staff age swordfish mainly by examination of annuli in cross-sections of anal fin spines and daily growth increments on sagittae using scanning electron microscopy. Results from mark-recapture operations are used to check the ageing procedures and validate the estimates of age and growth rates (DeMartini and Boggs, 1999). There remains some uncertainty with annuli deposition rates and false checks, which may account for discrepancies between the growth rate estimates of the NMFS and IOC laboratories (see Sun et al., 1999).

The annuli counts obtained at the Honolulu Laboratory are believed to be fairly representative of actual age, but the possibility of error is recognized. A subjective assessment of the plausible error associated with the identification of valid annuli was made with one of the principal investigators of the NMFS laboratory (J.H. Uchiyama). The results suggest that <5% of all annuli counts could be in error, with swordfish of ages 3-6 being easier to read than the younger or older fish (Table 2). However, additional uncertainty results from the process of estimating growth parameters from the available age-length data set. There are no data for fish beyond age-12, samples for age-1 are not representative of the catch due to gear selectivity, and there are apparent outliers in the data set. Consequently, some subjectiveness is needed to handle the data limitations.

To account for these two sources of uncertainty, the von Bertalanffy parameters were re-estimated using only a subset of the available data, which was modified before fitting the growth model. The data used consisted of length-age records for age groups 2 and above. For each fish in the data set, a possible age was selected at random using the Table 2 probabilities corresponding to the observed age of each fish. For cases where $T_0=0$, the L_∞ and K estimates were 226.46 and 0.253 for females and 197.686 and 0.290 for males.

The alternative estimates differ substantially from those proposed previously, which were considered as the best available. The alternative estimates translate into faster growth up to age-6, followed by slower growth up to a lower asymptotic size. Relying on this set of estimates for assessment purposes amounts to adding a process error. To provide insight into the effects of this type of error, the model allows the user to select the best or the alternative growth parameter values.

6. Spatial Structure

When a population is not exploited in proportion to abundance over its geographical range, movement must be accounted for to predict the effects of exploitation in one area on the abundance and catch rates in others. Given distribution data, an adequate spatial resolution must be selected for modeling. The latter is often dictated by the data attributes and the modeling objectives. The criteria used for selecting a particular spatial resolution, model, and distribution pattern are given below.

6.1 Distribution and movement

Commercial catch records indicate that swordfish occur throughout temperate, subtropical, and tropical waters, both in coastal and oceanic areas. The major determinants of migration patterns have been identified for many fresh water species (see Smith, 1985), but less is known about those of large pelagic species in the oceanic environment. For species like tuna and billfish, inferences are often made based on analysis of CPUE trends and release-recapture data. Standardized CPUE trends are not considered as accurate indicators of swordfish abundance for various reasons (Anon., 1999), and relatively few swordfish have been tagged, therefore information about the distribution and movement patterns of this species is fragmented and incomplete.

Bigelow et al. (1999) noted that oceanographers generally consider the North Pacific as composed of the subarctic domain north of 41°N , the subtropical domain around $20\text{-}30^\circ\text{N}$, and the North Pacific Transition Zone (NPTZ) between the two. The subarctic and subtropical frontal zones (SAFZ and STFZ) delineate these areas. The former occurs throughout the year at $40\text{-}43^\circ\text{N}$, and is associated with high swordfish CPUE in the Japanese fleet mainly at the confluence of the Oyashio and Kuroshio current extensions. The latter occurs in late fall to early summer at latitudes of $24\text{-}32^\circ\text{N}$ (Roden, 1991) and is associated with high swordfish CPUE in the Hawaiian fleet.

Bigelow et al. (1999) analyzed recent trends in swordfish CPUE in the Hawaiian longline fleet. Swordfish catch rates tend to be higher in spring and fall,

during full moon periods, in shallow waters (<1000 m), and at moderate sea surface temperatures (SST, 15-18°C.). Relatively high catch rates occur around fronts where water masses converge and generate greater primary and secondary productivity. Using satellite altimeter imagery, Seki et al. (1999) noted that sea surface height (SSH) varied by as much as 10 cm in the STFZ, with high spring catch rates occurring during low SSH. During such periods, the thermocline is close to the surface (50-100 m), and swordfish are thought to be at shallower depths and more susceptible to capture by longline gear. Seki et al. (1999) formulated a subtropical frontal index that explained 75% of the variation in swordfish CPUE during 1993-98. It is thus hypothesized that higher swordfish CPUE in the SAFZ and STFZ results from higher catchability due to stronger thermal stratification and that higher swordfish densities are stimulated by greater forage abundance.

Seki et al. (1999) hypothesized that the southward progression of high swordfish CPUE in spring-summer was evidence of a spawning migration. A recent analysis of swordfish CPUE trends in the Japanese longline fishery across the North Pacific supports the notion of a north-south migration but reveals no evidence of strong east-west migration during the year (P. Kleiber, pers. comm.). Berkeley's (1990) analysis of longline CPUE trends in the Atlantic also indicate extensive north-south movement, but very little east-west mixing.

There have been fewer analyses on swordfish distribution patterns in the southern hemisphere. Along the Australia coast, Ward (1996) noted there was a strong association between bigeye tuna and swordfish in longline catches of Japanese and Australian vessels along the southeastern Australian coast. Swordfish are caught primarily at latitudes of 25-34°S, in SST of 19-22°S during the full moon periods of June to October.

In terms of mark-recapture data, almost 500 swordfish have been tagged and released by the Hawaii-based commercial longline fleet. Of the 400 or so tagged north of Hawaii, three were recaptured 1-4 years later about 500 km from their point of release. Two others were recaptured 9 and 20 months later, about 1600 km and 3400 km northeast of their release location. In 1978, 17 swordfish were also tagged in the Southern California Bight. Six of these were recaptured within 5 weeks, and none had moved farther than 50 km (DeMartini and Boggs, 1999). These results indicate that swordfish can remain in one region for long periods, and they can engage in extensive east-west movement at an average speed of $\approx 18 \text{ km} \cdot \text{d}^{-1}$. Berkeley (1990) noted that over 3000 swordfish had been tagged in eastern and western parts of the Atlantic. His analysis of tagging data indicated extensive north-south movement, continuous swordfish distribution from east to west, but very little east-west mixing. The author concluded there was a considerable degree of stock isolation and proposed considering the population as being composed of separate stocks for assessment and management purposes.

Additional information on vertical and horizontal movement of swordfish was obtained from ultrasonic telemetry operations (Carey and Robinson, 1981; Carey, 1990). These confirmed that swordfish undertake diel vertical migrations. During daylight periods, they often remain deep (400-600 m), and ascend to the surface (0-100 m) at dusk to feed. The fish tracked often drifted or swam with the current and tended to move rapidly when in transit and more slowly once they reached their

inshore or offshore position. Carey (1990) observed small swordfish (120 cm EFL) swimming at speeds of 1-3 knots, for a median speed of $3 \text{ km}\cdot\text{h}^{-1}$ or $0.83 \text{ m}\cdot\text{s}^{-1}$, 1.4 body length per second, and $72 \text{ km}\cdot\text{d}^{-1}$. Carey (1990) observed larger swordfish (170 cm EFL) to swim at speeds of 2-4 knots for a median speed of $5 \text{ km}\cdot\text{h}^{-1}$ that corresponds to about $1.3 \text{ m}\cdot\text{s}^{-1}$, 1.3 body lengths per second, and $120 \text{ km}\cdot\text{d}^{-1}$. By comparison, Brill et al. (1999) predicted median speeds of about $1.04 \text{ m}\cdot\text{s}^{-1}$ and $1.25 \text{ m}\cdot\text{s}^{-1}$ for 120 and 170 cm yellowfin tuna (*Thunnus albacares*). These speeds are similar to those reported for swordfish of the same size.

The swordfish tracked by Carey (1990) usually followed the coastline while inshore. They also tended to move offshore on the surface at night and inshore and deep during the day. This pattern may be typical of fish in proximity to coastlines, but swordfish in the open ocean may not have similar reference points or access to forage areas near banks. It is assumed here that the latter travel comparable distances in a day but in various directions.

6.2 Spatial stratification

The initial focus of this model is on relatively large regions that may be subject to fishery management regimes in the future. Consequently, a high degree of spatial stratification is not required at this stage. The level of stratification chosen should be minimal to maximize computational efficiency. It should also account for the main features of the Pacific that are thought to affect swordfish distribution and help reveal latitudinal and longitudinal gradients in swordfish densities that may be indicative of recruitment patterns, migration routes, and exploitation effects. The preliminary stratification pattern was chosen after consultation with NMFS scientists involved in swordfish research (Fig. 10). It was considered to be a good compromise between excessively complex or overly simplistic stratification patterns. The rationale for selecting this pattern is presented below.

Swordfish are not often caught in the Pacific north of the 46th parallel, so the northernmost fishing ground is the region extending from the SAFZ to that parallel. Another is the STFZ. A third, less productive area lies between these two and covers most of the NPTZ. For purposes of convenience, each of these covers 7° in latitude from 25°N . South of this parallel lies a vast area between the STFZ and the equator. This southern region is considered as the only spawning ground and the only recruitment area for age-1 fish, so it was separated from the northern regions.

The SAFZ and STFZ extend across the Pacific. It seemed desirable to separate the eastern and western parts of the Pacific to show further gradients in exploitation impacts, so the large central regions are split into their eastern and western segments at 170°W . Furthermore, since coastal conditions differ from oceanic conditions, further distinction was made for the coastal regions in the northern part. Consequently, the North Pacific is separated into 10 regions that are not all of the same size (Table 3). This stratification level is similar to that used by Nakano (1998, Fig. 3) for assessing the status of swordfish in the North Pacific.

6.3 Selection of horizontal movement model

Turchin (1998) described various approaches used to model movement of plants and animals, while Sibert et al. (1999) gave a brief review of those commonly used for tuna stock-assessment. The latter authors noted that advection-diffusion models are best suited for cases involving strata that are not discretized, such as when predicting tag recoveries at any time and space. Simpler bulk transfer models, are suitable for cases involving large arbitrary regions. They are easily implemented in computer code and have parameters that can be estimated from tagging data. The bulk transfer method was used by Kleiber and Hampton (1994) to model the movement of tagged tuna around fish aggregating devices (FADs) through time. The authors noted that their approach was mathematically equivalent to the application of an advection-diffusion model in a spatially and temporally discretized context. Movement is regulated by transfer coefficients assigned to area boundaries facing north, south, east, and west. The authors used tagging data to estimate the transfer coefficients. Since the objective here is to quantify movement between arbitrarily defined regions and arbitrary time steps, a bulk transfer model is used. In the absence of an extensive mark-recapture data set, miscellaneous observations are used to formulate a general hypothesis about movement and to set the exchange rates across regions.

6.4 Horizontal movement hypothesis and parameterization

It is hypothesized that swordfish seek optimal temperatures to maintain physiological efficiency and frontal zones to maximize foraging success. Their search for optimal temperatures leads them north during the spring and south during fall along SSTs of 15°-18°C. Currents and gyres affect the distribution of plankton, the squid that feed upon them, and swordfish that prey on the latter. So movement from one region to the next is considered a function of SST, current and swimming velocities, region sizes, and the length of the boundaries crossed.

In regions 2 and 6 above the 35th parallel, the prevailing currents push swordfish eastward. Then the currents move swordfish southward along the California coast (region 10), westward below the 20th parallel (region 5 and 9), and northward along the Japan coast (region 1). Average velocities are about 5 cm·s⁻¹ for the North Pacific Current, 10 cm·s⁻¹ for the North Equatorial Current (Peixoto and Oort, 1992), 20 cm·s⁻¹ for the California Current, and 200 cm·s⁻¹ for the Kuroshio Current (Smith, 1976). This amounts to about 4.3, 8.6, 17.3, and 173 km·d⁻¹ respectively. Mean current velocities across the boundaries 1-2, 1-3, and 5-1 are assumed to be 170, 40, and 150 km·d⁻¹, respectively.

Swordfish can enter adjacent regions when moved by currents, or while swimming in search of better foraging conditions. In the absence of environmental effects, it is assumed that there is an equal probability that swordfish head north, west, east, and south while swimming. An average swordfish (150 cm EFL) is expected to cover 100 km·d⁻¹, or about 25 km·d⁻¹. Movement in any direction is reduced when swimming against the current and increased when going with it. Thus, a swordfish in region 6 is expected to travel about 29 km·d⁻¹ when moving eastward and 21 km·d⁻¹ when moving westward (Table 4). Current speeds at boundaries 5-1

and 1-2 (from origin to destination) exceed the hypothesized swimming speeds, so swordfish movement across these boundaries is considered to be insignificant.

SST response is accounted for by restraining swordfish from entering unfavorable regions. Mean monthly SST values for each region were computed from the 1984-97 Pathfinder AVHRR SST Monthly Mean Climatology (Casey and Cornillon, 1999). For each region/month stratum, a temperature score was assigned and used to compute a temperature gradient index that reflects the level of desirability of crossing the boundary between a region of origin and one of destination

$$(6.4.1) \quad q_o = \frac{|SST - 16.5|}{13} .$$

$$(6.4.2) \quad \nabla_{od} = \frac{1}{1 + e^{-10(0.5 + q_o - q_d)}} .$$

The above formulation assigns a score of zero to strata with the preferred SST of 16.5°. This score increases linearly to 1.0 as the SST drops to 3.5°, or increases to 29.5°. A gradient index of almost 1.0 (unrestrained movement) is obtained for a boundary separating regions with equal temperature scores, or when the region of destination has a higher score (more favorable conditions). A gradient index of 0.8 (slightly restrained movement) is obtained when moving from a region with a SST of 14.5° to another of 12°. The index is near zero (almost no movement) at a boundary separating regions with preferred and extreme SSTs. The model is not yet structured to accept exogenous input on oceanographic conditions to condition movement rates.

The term dispersal rate is used to designate the fraction of the population in one region that enters an adjacent one because of the combined effects of currents, swimming patterns, and behavioral responses to temperature gradients. A daily dispersal rate is computed from

$$(6.4.3) \quad u_{od} = \frac{V_{od} B_d \nabla_{od}}{W_o B_o} .$$

Not all regions share their entire boundaries with adjacent ones, which explains the need to account for boundary lengths in the above equation. For instance, when fish move north from region 5, only a fraction of these enter region 4, whose boundary overlaps partly with that of region 5.

In the absence of SST gradient effects, the predicted dispersal rates are not constant, reaching about 3%·d⁻¹, with most being less than 1%·d⁻¹ (Table 5). Simulations revealed that if dispersal is regulated only by SST gradient effects (omit factors V, W, B), the resulting coefficients cause the population to increase in regions 2-6 during the fall, in 3-7 during May-June, and in 4-8 during March-April, which correspond roughly to the distribution of SST in the 15°-18° range. However, the combination of all factors allows for unequal dispersal rates across time/area strata. Interestingly, Sibert et al. (1999) showed that skipjack tuna (*Katsuwonus pelamis*) also exhibited considerable spatial variability in directed and random movement.

Since the model accounts for mortality after the movement of fish across regions, the number of fish in each time/region stratum is considered to be simply a function of previous abundance, recruitment, immigration, and emigration

$$(6.4.4) \quad N_{jot+1} = N_{jot} + R_{jot} - \sum_{d=1}^{D_o} (N_{jdt} \mathbf{u}_{do} + N_{jot} \mathbf{u}_{od}) .$$

Prior to each monthly fishing incident, the numbers of fish by age group in each region are updated by applying the same dispersal rates to all age-4+ fish. For younger groups, movement is allowed only between southern regions (5, 9, 4, 8) since it is hypothesized that small swordfish do not have sufficient mass to maintain the thermal inertia required to forage extensively in cold water regions and depths (E. DeMartini, pers. comm.). Recruitment of age-1 fish is allowed only in the southmost regions where spawning occurs, with 70% of the recruitment going to region 5 and 30% to region 9, as if a portion of the recruits drift westward during their first year before moving to other regions. The equatorial region has been characterized as having high productivity throughout the year (Chavez and Barber, 1987) and has been characterized as a region of feeding and growth for immature swordfish (Kume and Joseph, 1969).

Because of the unequal exchange rates across regions, the predicted densities increase in some regions and decrease in others, and stabilize at some relatively stable level after a few iterations (< 30 d). Simulations conducted in the absence of exploitation ($F=0$) revealed that the predicted densities (biomass·km⁻²) tended to be higher in the western Pacific (regions 1-5) than in the eastern Pacific (regions 6-10). Predicted densities are highest in regions 3-4 and are about three times greater there than in the lowest density region in the south (region 5). Thus, the predicted density patterns conform surprisingly well to the swordfish CPUE trend of the Japanese longline fishery, which is highest in the zone of peak densities. Given such results, there is no need to add a density-dependent component to the model to prevent unrealistically high densities from occurring in some regions.

7. Testing of Assessment

Before the model could be used to assess the performance of stock-assessment procedures, it was ensured that the function predictions were accurate and realistic. A series of tests was conducted for this purpose. This involved comparing the outputs of the various C++ functions to those of equivalent functions in the form of FORTRAN77 programs, Microsoft Excel spreadsheet templates, numerical library routines, and commercial applications used for statistical analysis (SPSS, S-PLUS, STATISTICA, etc.). The model was also supplied with various types of erroneous input values to ensure that these would be detected and that program execution would halt. The population was also subjected to relatively severe conditions (high exploitation, low temperatures, high natural mortality rates, etc.) to determine if the time series of predicted density trends appeared plausible under such conditions.

After completing these tests, NMFS staff began using the operational model as an analytical tool to determine the performance assessment procedures used at the Honolulu Laboratory. At the time of this writing, only a single assessment

procedure had been tested with the operational model. This consisted of a slightly modified Pella-Tomlinson nonequilibrium production model used to conduct a preliminary assessment of swordfish stock status in the North Pacific (see Kleiber, 1999a). This production model was coded as an AD Model Builder template (Fournier, 1996), which is a framework for model building that uses an automatic differentiation algorithm to optimize the objective function (see Quinn and Deriso, 1999; p. 354). The results of the production model analysis suggested that the North Pacific population had been subjected to relatively low exploitation. However, the results were not considered to be very reliable, as the nature of the factor responsible for this could not be determined with certainty (Kleiber, 1999a). The main factors suspected included errors in the time series of catch and effort, lack of contrast in the data, model misspecification, and malfunction of the parameter estimation procedure.

To help determine the factor(s) responsible for the assessment failure, the operational model was used to generate several sets of catch and effort statistics that served as input to the production model. After each production model analysis, the results were compared to the known values used to generate the data. Initially, 45-year time series catch and effort data were generated for a very simple swordfish fishery. Data sets were then generated for progressively more complex fisheries, such that the final scenario resembled the actual situation in the North Pacific.

The base case represents a simplistic scenario. Growth and spawning patterns conformed to the hypothesized patterns described in the text. Natural mortality rates (M) were set to 0.15yr^{-1} for females and 0.43yr^{-1} for males. The Ricker type stock-recruit function was used to predict recruitment, but no stochasticity in recruitment was allowed. All age-1 recruits were distributed across the 10 regions in proportion to region size. No movement of fish between regions was allowed after recruitment. No Allee effects were allowed for, so the population can rebuild at maximum rates even after severe depletion. The catchability coefficient was held fixed during the 45-year period, and all age groups were equally susceptible to harvest (no gear selectivity effect). Fishing effort for a single longline fishery was distributed across all regions in proportion to region size. Fishing effort index was increased progressively to reach 181 times the initial value by year 20 and then reduced progressively to the starting value. This caused the biomass to drop to 50% of its initial size and then bounce back, which provided relatively high contrast in the catch-effort series. Because of the effort distribution pattern used, there was no need to standardize effort with Honma's (1974) method before analyzing the effort series. The catch and effort values generated imply that there are no deficiencies in sampling coverage, and there are no observation errors.

The values computed for testing the production model consisted of the starting population size (N_0), the carrying capacity ($K = N_0$) considered as fixed, the intrinsic rate of increase (r), the production ogive shape parameter (m), the fishery catchability coefficient (q), the maximum sustainable yield ($MSY = rK/4$), biomass-at- MSY ($MSY_b = K/2$), harvest rate at MSY ($MSY_h = r/2$), and effort at MSY ($MSY_f = r/2q$). The intrinsic rate of increase (parameter r) of the population was determined with the operational model by reducing the virtual swordfish population to 5% of its original size through intense exploitation, then letting the population recover in the absence of fishing mortality. Parameter r is then given by the maximum slope of the

abundance trend as the population size increases. Given r , q , and K , the other parameters can then be computed directly.

The production model analysis was then conducted with 12 steps per year, and equal penalty weights were assigned to the residual deviations for carrying capacity, catchability, and effort values (see Kleiber 1999 for details). For the base case, the estimates obtained were relatively close to the actual values (Table 6). Further simplification of the base case resulted in estimates that were almost identical to the 'known' values used to generate the data. This observation supports the notion that (i) the operational model had little (or no) coding errors such that the numbers predicted are accurate, (ii) the production model algorithm is also correct, and (iii) the underlying function minimization procedure of AD Model Builder performed well.

Additional complexity was then added to the base case scenario. For case #2, the single fishery was replaced by two identical fisheries (so two catchability coefficients are estimated), each with half of the original effort level but with identical spatial distribution of effort and catchability coefficients. For case #3, the activity of the second fleet was restricted to the last 7 years of the 45-year period. All of the original effort was allocated to the first fishery during the first 38 years, with effort split between fisheries during the last 7 years. Case #4 is the same as #3, except that fishing intensity was lower such that original biomass was reduced by only 28% during the simulation period, for a substantially less contrast in the catch-effort series. For case #5, all of the original effort was assigned to the first fishery, and the second fishery expanded from zero to the same level as the first during the last 7 years. For case #6, the spatial distribution of effort was changed, such that effort for the second fishery was deployed only in regions 8, 9, and 10 in proportion to region size. It should be noted that despite the additional complexity, the production model still yielded estimates that were within 40% or so of the actual values.

For case #7, recruitment conformed to the hypothesized pattern, and movement of fish across regions was enabled. These modifications led to a change in the dynamics of this population, its intrinsic rate of increase, and its overall productivity. Consequently, a new set of known values served as targets, and the parameters were estimated using 24 steps per year. Relatively accurate results were still obtained despite the additional complexity (Table 6). For case #8, the area of activity of the first fleet was allowed to expand every 5 years such that by year 15 all regions were subjected to fishing activity. Under this scenario, unrealistic parameter estimates were obtained (Table 6).

It was hypothesized that the progressive expansion of fishing operations into previously unfished areas yields catch-effort series by time/area that show different CPUE trends. The process of aggregating these into annual figures results in 'noisy' catch-effort series that the production model has difficulty interpreting properly. In such situations, it would seem preferable to rely on a more sophisticated assessment procedure that processes data in a spatially disaggregated fashion. In the absence of such procedures, for case #9 we attempted to minimize this problem by using only a subset of the data so as to eliminate the effect of the spatial expansion of activity. In this case, only the catch-effort series generated for regions 1-4 was supplied to the production model. This failed to provide realistic estimates (Table 6).

For case #10, an alternative approach was used to eliminate the same problem. Here again, this involved using a subset of the 45-year catch-effort data set, but rather than restricting the series spatially it was restricted temporally, such that only the last 34 years of the aggregated catch-effort data set were used as input to the production model. The results now agree to a much greater extent with the known values, despite having a shorter time series with less contrast (Table 6). Case #11 is the same, except gear selectivity was allowed for with the same selectivity for both longline fisheries. For case #12, stochastic variation in recruitment was allowed for in accordance with the hypothesized pattern (see previous section). Note that case #12 now represented a realistic fishery scenario, except for the absence of errors such as deficiencies in catch monitoring, misreporting, and observation errors. Under such conditions, the parameter estimates still tended to be within about 50% of the true values, which is considered relatively good for this type of assessment. Finally, for case #13, effort was standardized with the Honma's (1974) method, but did not lead to substantial improvements in the parameter estimates.

Cases 12-13 represented scenarios that are similar to the North Pacific swordfish fishery when taking into account only the activities of the Japanese and U.S. longline fishing operations. The actual production model analysis conducted by NMFS staff at the Honolulu Laboratory also accounted for catches by Asian drift gillnet fleets (Kleiber, 1999a). However, as noted earlier, the production model analysis did not yield satisfactory results. In light of the test results obtained, it was reasoned that more reliable estimates might be obtained by eliminating the first 11 years of data since the post-war expansion of fishing activity by the Japanese fleet was largely over by 1962 (see Ward, 1996; p. 9). So a production model analysis was repeated under such conditions. The analysis was also repeated without the inclusion of Asian drift gillnet catches and finally without the Honma standardization. Neither one of these analyses yielded results that were considered better or more reliable. It was concluded that the assessment failure was likely due to a data failure (Hilborn and Walters, 1992), expressed as either a lack of sufficient contrast in the actual catch-effort series, errors in the catch-effort series, non-availability of standardized effort series for the drift gillnet fleet, and omission of other ancillary catches (harpoon, recreational, Mexican longline, etc.) from the analyses. Current plans are to repeat the production model analysis and the associated tests with improved data sets once these become available.

8. Model Forecasts

The assessment failure described in the previous section created a need to find an alternative assessment procedure for this data poor context. In the absence of a clearly superior alternative an attempt was made to use the operational model to gain further insight into the exploitation potential of the North Pacific swordfish population. With this approach in mind, catch and effort statistics for various fisheries in the Pacific were first compiled to reconstruct the exploitation history. The Japanese data were provided to the NMFS Honolulu Laboratory by the National Research Institute of Far Seas Fisheries (NRIFS) Laboratory in Shimizu, Japan. These data covered the 1952-96 period and were stratified by year and area. The U.S. data covered the 1990-96 period and were stratified by year, month, and area. In both cases, each area stratum covered 5° in longitude by 5° in latitude. Catch and effort measures were the number of swordfish caught and the number of hooks

deployed. The catch and effort data were converted to a different format (year/month/region) by uniformly distributing the annual Japanese effort over 12 months each year and pooling the area statistics into the corresponding regions (1-10) as used by the model.

Sakagawa (1989) noted that during 1952-1962, the Japanese longline fishery targeted swordfish and albacore by deploying the gear at night in shallow sets using squid as bait. Then the fishery started targeting various tuna species for sashimi markets and switched to daytime sets using several bait types. Uozumi and Yokawa (1999) noted that the coastal longline fleet did not adopt the nylon longline gear used in offshore and distant fleets and remains a traditional swordfish directed fishery. A second major change in the Japanese longline fishery began in 1975, with the progressive deployment of longline gear having more hooks per basket to target bigeye tuna at greater depths (Suzuki et al., 1977). By comparing catch rates of shallow and moderately deep sets (50-120 vs. 50-250 m) in the WCPO during the late 1970s, they showed that swordfish catch rates were about 25% lower in deeper sets. Nakano (1998) also noted that swordfish CPUE in the Japanese longline fishery decreased when fishing gear was set deeper. It is thus hypothesized that the major changes in longline fishing operations led to a reduction in swordfish catchability.

To account for such changes, scientists often standardize effort series by means of Generalized Linear Models (GLM, McCullagh and Nelder, 1989) or Generalized Additive Models (GAM, Hastie and Tibshirani 1990) before predicting catch trends. Simpler methods such as proposed by Hinton and Nakano (1996) have also been used to account for differences in the vertical distribution of fish and that of the longline gear. However, the information required for standardizing the effort series with these methods was not available to the author at the time of this writing. So these changes are simply accounted for in the model by reducing the baseline catchability coefficient of the Japanese longline fleet by $25\% \cdot \text{yr}^{-1}$ during 1962-1964, and by $2\% \cdot \text{yr}^{-1}$ from 1975 onwards. These rates were subjectively chosen based on a visual examination of various standardized effort series reported in the literature.

By contrast to the Japanese fishery, the US longline fleet is relatively young. The Hawaiian longline fleet is much larger than any other U.S. island-based fishery in the western Pacific and was described by Boggs and Ito (1993), and Bigelow et al. (1999). Most vessels in this fleet target swordfish, by deploying 50-60 km lines with 3-6 hooks per basket. The lines are deployed at night around the new moon period. Sets are made such that the bait (usually squid) lies 30-90 m under the surface. Yellow-green lightsticks are attached to some gangions (20-100% of them) to attract large pelagic fishes to the bait. A cursory examination of the U.S. longline catch rates indicated that they tended to be higher (0-15x) than those of Japanese vessels operating in the same time/area stratum. On closer examination, it was noticed that the increased efficiency of the U.S. vessels was greatest above the 25th parallel. To account for this observation, the catchability coefficient of the US longline fleet was set to 4 times that of the Japanese fleet in regions 5 and 9 and 8 times higher in other regions at corresponding times.

Swordfish are also caught in other North Pacific fisheries, whose catch and effort statistics are not as readily available to NMFS staff and are characterized by a

greater level of uncertainty and incompleteness than the Japanese and U.S. statistics. Still, efforts were made to compile them to account for most of the exploitation process. Catch and effort data for the Taiwanese and Korean longline fisheries for 1967-92 were extracted from NMFS databases. A cursory examination of these data indicated that effort was deployed predominantly in the regions 5 and 9 and that the efficiency of these fleets was less than that of the Japanese fleet across most strata. The swordfish catchability of the Korean and Taiwanese fleets was set to 18% of the Japanese fleet for 1967-80 and to 33% for 1981 onward. Catch and effort statistics for 1993-96 were not available, so these were assumed to be comparable to the 1992 levels.

Swordfish are also caught in harpoon, drift gillnet, and recreational fisheries on both sides of the North Pacific. The 1970-93 catches in coastal waters off California were reported by Holts and Sosa-Nishizaki (1998). The corresponding Japanese and Taiwan statistics were reported by Sakagawa (1989) and Uozumi and Yokawa (1999). The available Mexican longline and drift gillnet catches were incomplete and represented a relatively small portion of total catch and effort statistics. Consequently, the catch and effort statistics for the Mexican fisheries were omitted from the present analysis. Catches for other fisheries reported on an annual basis were distributed uniformly across months. All catches in harpoon, drift gillnet, and recreational fisheries were added to those of longline fisheries in the corresponding strata, and longline effort in these strata was increased proportionally. This translation of harpoon, drift gillnet, and recreational effort into longline effort equivalencies was done for purposes of simplification and to facilitate computation of yield versus effort. The catchability coefficient in the pseudo-longline fishery was set to 70% that of the Japanese longline fishery in the corresponding strata, and a type II curve (Fig. 4) was used to describe selectivity in this fishery. This combination of gear selectivity and catchability coefficient resulted in predicted catch levels that were commensurate with those observed in the combination of drift gillnet, harpoon, and recreational fisheries. Catch and effort data in these fisheries for 1993-96 were not available, so these were assumed to be identical to the 1993 levels.

The operational model was used to predict total annual catches (in pieces), first using only the Japanese and U.S. longline fishing effort and then using effort for all fisheries. The baseline annual M for females was set to 0.15. The differential mortality option was selected. The baseline catchability coefficient used for the Japanese fleet was set to 0.03 for region 10. The catchability coefficients for other regions were adjusted in proportion to region size relative to that of region 10. The Ricker stock-recruit function was selected, and stochastic variation in recruitment was allowed for. Movement of fish across regions and the two gear selectivity options were enabled. No other observation or process errors were allowed. The model's user interface is shown in Appendix III, along with the sequence of options selected for this run (9 2 0 0 0 0 0 1 1 0 0 0 0 0).

The predicted catch trends conformed well with the observed patterns (Fig. 11, 12), when using a low baseline catchability coefficient that gave annual fishing mortality rates ranging from 0.004 to 0.011. This coefficient can be increased to explore the hypothesis that the historical fishing mortality trend was higher than this level and determine the long-term yields associated with particular effort levels. This was done by increasing the simulation period to 150 years and maintaining effort

levels for years 46-150 at the 1996 level. Beyond year 45, predicted catches fluctuated for several years and then progressively stabilized at some level, so the predicted yield for a given effort level was set to the average over the last 20 years. For each baseline catchability coefficient, the predicted CPUE trend over the first 45 years was compared to the observed trend, and the best fitting series was considered as being the most representative of the actual effort series. The effort level associated with the 1996 catch was labeled as 1x, and all yield-effort relations were expressed as functions of the 1996 values.

The predicted maximum long term yield (LTY) was associated with a relative effort index of about 13 times the 1996 effort level (Fig. 12). Predicted overall fishing mortality rate (F_{msy}) at the LTY level is about 0.26, which corresponds roughly to the average natural mortality rate for males and females used in the simulation. The 1996 swordfish catch in the North Pacific was about 14,000 mt (Anon., 1999), representing about 40% of total swordfish catches in the entire Pacific ocean (Folsom et al., 1997). Assuming that total fishing effort in 1996 is equivalent to the 1x level, the 1996 yield would have been about 24% of the LTY, which would be about 57,000 t. This LTY is considered plausible and exceeds the peak North Pacific swordfish catch in 1960 of about 38,000 t. However, there is considerable uncertainty around this figure, and its associated confidence intervals cannot be computed in a conventional manner. In light of this, the above figures should be considered only as crude indicators of potential yield.

If one considers the LTY as analogous to MSY, several reference points (see Smith et al. 1993) can be computed using the criteria proposed by Restrepo et al. (1998). Given an MSY of 57,000 t, and an F_{msy} of 0.26, biomass at MSY (B_{msy}) is estimated to be about 219,000 t. Using a relative effort index of 1x, the fishing mortality rate in 1996 (F_{96}) is predicted to be about 0.0254 for an F_{96}/F_{msy} of about 0.1. The 1996 biomass ($B_{96} = '96 \text{ catch} / F_{96}$) is about half a million t. The minimum stock size threshold (MSST) computed from proxies for 'data-moderate' species is about half of MSY or about 111,000 t. Since B_{96} exceeds MSST and F_{96}/F_{msy} is less than 1.0, the North Pacific swordfish population is not considered to be overexploited. This observation is in agreement with the results of the production model analysis, which suggested that this population had been subject to relatively low exploitation rates so far. However, it is recognized that agreement between the results of two independent analyses constitutes only limited support for the low exploitation hypothesis, and there is a need to revise this assessment once new information becomes available.

9.0 Conclusion

The application of conventional stock-assessment methods often requires considerable information on the demographic traits of the fish stock(s), the effort distribution by gear types and fisheries, and the catch rates and composition by strata. When crucial information is lacking, investigators can resort to overly simplistic models to assess stock status using only subsets of existing data. The results presented here show that an operational model is a useful compromise between these extremes in that it can utilize all existing data and can be used to make predictions that are comparable with the time series of observations. The predictions can also be compared with those generated with other models to provide

further insight into the dynamics of the system, the limits of the data, and the performance of other estimators.

The test results presented show that the production model tested performed relatively well under a variety of conditions, but failed to provide reliable estimates of the management parameters of interest under conditions that are more realistic. Further insight into the productive capacity of the North Pacific population was obtained by using the operational model as a forecasting tool. The model was not primarily designed for this purpose, and the reliability of the predictions remains to be proven. Still, the exercise highlights the potential usefulness of the operational model in data poor contexts, which could increase if additional efforts are made to improve the components of the model to account for new information on this stock and the supported fisheries.

10. Citations

- Allee, W.C., A.E. Emerson, O. Park, T. Park, and K.P. Schmidt. 1949. Principles of Animal Ecology. Saunders, Philadelphia. 837 pp.
- Anonymous. 1999. Report of the Second Meeting of the Interim Scientific Committee on tunas and tuna-like species in the North Pacific (ISC). Honolulu, HI, USA. Plenary session Jan. 20-23, 1999.
- Arocha, F. 1997. The reproductive dynamics of swordfish *Xiphias gladius* L. and management implications in the northwestern Atlantic. Ph.D. Thesis. Univ. of Miami. Rosenthal School Marine and Atmospheric Sciences. Coral Gables. Florida, USA. 383 p.
- Arocha, F., and D.W. Lee. 1995. Maturity at size, reproductive seasonality, spawning frequency, fecundity and sex ratio in swordfish from the northwest Atlantic. ICCAT/SCRS/95/98.
- Anonymous. 1997. National Marine Fisheries Service Southwest Fisheries Science Center Honolulu Laboratory Program Review. U.S Dept. Comm. NOAA. October 1997. 131 p.
- Berkeley, S. A. 1990. Trends in Atlantic swordfish fisheries. P. 47-80 *In* Proceedings of the Second International Billfish Symposium. Part I. Kailua-Kona, HI, USA. August 1-5. 1988. R.H. Stroud (ed.). 361 pp. National Coalition for Marine Conservations Inc. Savannah, Georgia.
- Beverton, R. J. H., and S. J. Holt. 1957. On the dynamics of exploited fish populations. Fisheries Investment Series 2, Vol. 19. U.K. Ministry of Agriculture and Fisheries, London.
- Bigelow, K. A., C. H. Boggs, and X. He. 1999. Influence of environmental factors on swordfish and blue shark catch rates in the U.S. North Pacific longline fishery. Fishery Oceanography.
- Boggs, C. H. 1989. Vital rate statistics for billfish stock assessments. P. 225-233 *In* Proceedings of the Second International Billfish Symposium. Part I. Kailua-Kona, HI, USA. August 1-5. 1988. R. H. Stroud (ed.). 361 pp. National Coalition for Marine Conservations Inc. Savannah, Georgia.
- Boggs, C.H., and R. Ito. 1993. Hawaii's pelagic fisheries. Marine Fisheries Review. 55(2): 69-82.
- Breymann, U. 1998. Designing components with the C++ STL. A new approach to programming. Addison-Wesley. New York, USA. 307 pp.
- Brill, R. W., B. A. Block, C.H. Boggs, K.A. Bigelow, E.V. Freund and D.J. Marcinek. 1999. Horizontal movements and depth distribution of large adult yellowfin tuna (*Thunnus albacares*) near the Hawaiian Islands, recorded using

ultrasonic telemetry: implications for the physiological ecology of pelagic fishes. *Marine Biology* 133: 395-408.

- Caddy, J. F. and R. Mahon. 1995. Reference points for fisheries management. FAO Fisheries Technical paper No. 347. 83 pp.
- Campbell, R., A. Punt, and T. Smith. 1998. Evaluation of performance indicators in the Australian eastern tuna and billfish fishery. Working paper presented at the Workshop on Precautionary Limit Reference Points for Highly Migratory Fish Stocks in the western and central Pacific ocean. Honolulu, HI, USA. 28-29 May, 1998. *In* Report of the 11th meeting of the Standing Committee on Tuna and Billfish. Secretariat of the Pacific Community. Noumea, New - Caledonia.
- Carey, F. G. 1990. Further acoustic telemetry observations of swordfish. P. 103-122 *In* Proceedings of the Second International Billfish Symposium. Part II. Kailua - Kona, HI, USA. August 1 -5. 1988. R. H. Stroud (ed.). 361 pp. National Coalition for Marine Conservations Inc. Savannah, Georgia.
- Carey, F.G., and B.H. Robinson. 1981. Daily patterns in the activities of swordfish, *Xiphias gladius*, observed by acoustic telemetry. *Fish. Bull.* 79: 277-292.
- Casey, K. S., and P. Cornillon. 1999. A comparison of satellite and in situ based sea surface temperature climatologies. *Journal of Climate*. 12(6): 1848-1863.
- Chavez, F. P., and R. T. Barber. 1987. An estimate of new production in the equatorial Pacific. *Deep-Sea Res.* 34(7): 1229-1243.
- DeMartini, E. E., and C. H. Boggs. 1999. Biological research in support of swordfish stock assessment. Second meeting of the Interim Scientific Committee for Tuna and Tuna-like species in the North Pacific Ocean (ISC). Jan. 15-23, 1999. Honolulu, HI, USA. ISC2/99/SFWG/3.
- DeMartini, E. E., Uchiyama, J.H., and H.A. Williams. (in prep.). Sexual maturity, sex ratios, and size composition of swordfish caught by the Hawaii-based pelagic longline fishery. *Fish. Bull.*
- Folson, W. B., D. M. Weidner, and M. R. Wildman. 1997. World swordfish fisheries. An analysis of swordfish fisheries, market trends, and trade patterns *Past-Present-Future*. Volume I. NOAA Tech. Memo. NMFS-F/SPO-23. 50 p.
- Fournier, D. A. 1992. AUTODIFF. A C++ array language extension with automatic differentiation for use in nonlinear modeling and statistics. Otter Research Ltd., Nanaimo, BC Canada. 56 p.
- Fournier, D. A. 1996. An introduction to AD Model Builder for use in nonlinear modeling and statistics. Otter Research Ltd., Nanaimo, BC Canada. 56 p.
- Fournier D. A., J. R. Sibert, J. Majkowski, and J. Hampton. 1990. MULTIFAN a likelihood-based method for estimating growth parameters and age

composition from multiple length frequency data sets illustrated using data for southern bluefin tuna (*Thunnus maccoyii*). Can. J. Fish. Aquat. Sci. 47, 301-317.

- Garcia-saez, C. 1996. Assessing populations of swordfish from the North Atlantic: Density dependence, maximum sustainable yield levels and size-classified demographic models. ICAAT SCRS/96/143. P. 345-358.
- Goodyear, C. P. 1989. LSIM - A length-based fish population simulation model. U.S. Dept. Commerce. NOAA Technical Memorandum NMFS-SEFC 219. 55 pp.
- Graal, C., D. P. De Sylva, and E. D. Houde. 1983. Distribution, relative abundance and seasonality of swordfish larvae. Trans. Am. Fish. Soc. 112: 235-246.
- Hastie, T., and R. Tibshirani. 1990. Generalized Additive Models. Monograph on Statistics and Applied Probability 43. Chapman and Hall, London. 335 p.
- Hilborn R., and C. J. Walters 1992. Quantitative Fisheries Stock Assessment. Chapman and Hall, New York, NY, USA, 570 p.
- Holling, C.S. 1959. Some characteristics of simple types of predation and parasitism. Canadian Entomologist, 91, 385-398.
- Holts, D., and O. Sosa-Nishizaki. 1998. Swordfish, *Xiphias gladius*, fisheries of the eastern North Pacific Ocean. P. 65-76 *In* Papers from the International Symposium on Pacific swordfish, Ensenada, Mexico. 11-14 Dec., 1994. Barrett et al. (ed). NOAA Tech. Rep. NMFS 142. 276 pp.
- Honma, M. 1974. Estimation of overall fishing intensity of tuna longline fishery. Bull. Far Seas Fish. Res. Lab. (Shimizu) 10: 63-66.
- International Council for the Exploration of the Sea (ICES). 1993 Report of the Working Group on Methods of Fish Stock Assessments. ICES Cooperative Research Report No. 191. Copenhagen.
- IMSL, 1989. FORTRAN subroutines for mathematical applications. Math Library Version 1.1. IMSL Inc. Sugarland, Texas, USA, 1150 p.
- Hinton, M.G. and R. B. Deriso. 1998. Distribution and stock assessment of swordfish, *Xiphias gladius*, in the eastern Pacific ocean from catch and effort data standardized on biological and environmental parameters. P. 161-179 *In* Papers from the International Symposium on Pacific swordfish, Ensenada, Mexico. Dec. 11-14, 1994. Barrett et al. (ed). NOAA Tech. Rep. NMFS 142. 276 pp.
- Hinton, M. G., and H. Nakano. 1996. Standardizing catch and effort statistics using physiological, ecological and behavioral constraints and environmental data, with an application to blue marlin (*Makaira nigricans*) catch and effort data from the Japanese longline fisheries in the Pacific. IATTC Bull. 21(4):117-200.

- Kimura, D. K., and G. P. Scott. 1994. Length-based separable sequential population analysis as applied to swordfish (*Xiphias gladius*). ICCAT Collective Volume of Scientific Papers 42(1):85-96. Madrid.
- Kleiber, P. 1999a. A very preliminary North Pacific swordfish assessment. Second meeting of the Interim Scientific Committee for Tuna and Tuna-like species in the North Pacific Ocean (ISC). Jan. 15-23, 1999. Honolulu, HI, USA. ISC2/99/SFWG/2.2.
- Kleiber, P. 1999b. Critique of assessment methods and models - identification of data collection and research needs. P. 210-208 *In* Proceedings of the Second International Pacific Swordfish Symposium. DiNardo, G. T. (ed.) NOAA Technical Memorandum NMFS, June 1999. NOAA-TM-NMFS-SWFSC-263. 240 pp.
- Kleiber, P., and J. Hampton. 1994. Modeling effects of FADs and islands on movement of skipjack tuna (*Katsuwonus pelamis*): Estimating parameters from tagging data. Can. J. Fish. Aquat. Sci. 51: 2642-2653.
- Kume, S., and J. Joseph. 1969. The Japanese longline fishery for tunas and billfishes in the eastern Pacific ocean east of 130°W, 1964-1966. Inter-Am. Trop. Tuna. Comm. Bull. 13: 275-418.
- Labelle, M., J. Hampton, K. Bailey, T. Murray, D.A. Fournier, J.R. Sibert. 1993. Determination of age and growth of south pacific albacore (*Thunnus alalunga*) using three methodologies. Fish Bull. 91, 649-663.
- Labelle, M., T. Hoch, B. Liorzou and J. L. Bigot. 1997. Indices of bluefin tuna (*Thunnus thynnus thynnus*) abundance derived from sale records of French purse seine catches in the Mediterranean sea. Aquat. Liv. Res. 1997. 10(6): 329-342.
- Linhart, H., and W. Zucchini. 1986. Model selection. Wiley, New York.
- McCullagh P., and J. A. Nelder. 1989. Generalized Linear Models. Second edition. Monograph on Statistics and Applied Probability 37. Chapman & Hall. New York, U.S.A. 511 p.
- Meyers, S. 1997. Effective C++. Second Edition. Addison Wesley. Mass. USA. 256 p.
- Nakano, H. 1998. Stock status of Pacific swordfish, *Xiphias gladius*, inferred from CPUE of the Japanese longline fleet standardized using General Linear Models. P. 195-209 *In* Papers from the International Symposium on Pacific swordfish, Ensenada, Mexico. Dec. 11-14, 1994. Barrett et al. (ed). NOAA Tech. Rep. NMFS 142. 276 pp.
- National Research Council (NRC). 1998. Improving fish stock assessments. Committee on Fish Stock Assessment Methods. National Research Council. National Academy Press, Washington D.C. 1998. 176 p.

- Neter, J., W. Wasserman, and M. H. Kutner. 1985. Applied linear statistical models: Regression, analysis of variance, and experimental designs. Homewood, IL: Irwin.
- Nishikawa, Y., M. Honma, S. Ueyanagi, and S. Kikkawa. 1985. Average distribution of larvae of oceanic species of scombroid fishes., 1956-1981. Series 12. Far Seas Research Laboratory.
- Peixoto, J. P., and A. H. Oort. 1992. Physics of climate. American Institute of Physics. New York. USA. 520 p.
- Prager, M. H., C. P. Goodyear and G. P. Scott. 1996. Application of a surplus production model to a swordfish-like simulated stock with time-changing gear selectivity. Trans. Amer. Fish. Soc. 125:729-740.
- Press W. H., S. A. Teukolsky, W. T. Vetterling, B. P. Flannery. 1992. Numerical recipes. The art of scientific computing (2nd ed.). Cambridge University Press. Cambridge, U.K., 963 p.
- Quinn II, T. J and R. B. Deriso. 1999. Quantitative Fish Dynamics. 1999. Oxford University Press. New York. 542 pp.
- Restrepo, V. R., G. G. Thompson, P. M. Mace, W. L. Gabriel, L. L. Low, A. D. MacCall, R. D. Methot, J. E. Powers, B. L. Taylor, P. R. Wade, J. F. Witzig. 1998. Technical guidance on the use of precautionary approaches to implementing national standard 1 of the Magnuson-Stevens Fishery Conservation and Management Act. NOAA Technical Memorandum NMFS-F/SPO 31. 53 pp.
- Richards, L., J. T. Schnute and N. Olsen. 1997. Visualizing catch-age-analysis; a case study. Can. J. Fish. Aquat. Sci. 54: 1646-1658.
- Richards, L., and J. T. Schnute. 1997. Model complexity and catch-age analysis. Can. J. Fish. Aquat. Sci. 55: 949-957.
- Ricker, W. E. 1954. Stock and recruitment. J. Fish. Res. Bd. Can. 11: 559-623.
- Ricker, W. E. 1975. Computation and interpretation of biological statistics of fish populations. Bull. Fish. Res. Bd. Can. 191: 382 pp.
- Roden, G. I. 1991. Subarctic-subtropical transition zone of the North Pacific: large scale aspects and mesoscale structure. In: Biology, Oceanography, and Fisheries of the North Pacific Transition Zone and Subarctic Frontal Zone. NOAA Tech. Rep. NMFS SWFSC-105, p. 1-38.
- Sakagawa, G.T. 1989. Trends in fisheries for swordfish in the Pacific ocean. P. 61-79 *In* Proceedings of the Second International Billfish Symposium. Part I. R. H. Shroud (ed.). Kailua-Kona HI, USA. Aug. 1-5. 1988. 361 pp. National Coalition for marine conservation. Savannah, Georgia.

- Schnute, J. T. 1994. A general framework for developing sequential fisheries model. *Can. J. Fish. Aquat. Sci.* 51: 1676-1688.
- Schnute, J. T., and D. Fournier. 1980. A new approach to length frequency analysis: growth structure. *Can. J. Fish. Aquat. Sci.* 37: 1337-1351.
- Schnute, J. T., and L. J. Richards. 1995. The influence of error on population estimates from catch-age models. *Can. J. Fish. Aquat. Sci.* 52: 2063-2077.
- Seki, M. P., J. J. Polovina, D. R. Kobayachi, and B. C. Mundy. 1999. The oceanography of the Subtropical Frontal Zone in the central North Pacific and its relevancy to the Hawaii-based swordfish fishery. Working Document, Second Meeting of the Interim Scientific Committee for Tuna and Tuna-like species in the North Pacific (ISC). January 15-23, 1999. Honolulu, HI, USA.
- Sibert, J. R., J. Hampton, D.A. Fournier, and P. J. Bills. 1999. An advection-diffusion-reaction model for estimation of fish movement parameters from tagging data, with application to skipjack tuna (*Katsuwonus pelamis*). *Can. Jour. Fish. Aquat. Sci.* (56: 925-938).
- Skillman, R. 1998. Central Pacific swordfish, *Xiphias gladius*, fishery development, biology, and research. P. 101-124 *In* Papers from the International Symposium on Pacific swordfish, Ensenada, Mexico. Dec. 11-14, 1994. Barrett et al. (ed). NOAA Tech. Rep. NMFS 142. 276 pp.
- Smith, J. S., J. J. Hunt, and D. Rivard. 1993. Risk evaluation and biological reference points for fisheries management. *Can. Spec. Publ. Fish. Aquat. Sci.* 120: 440 pp.
- Smith, R. L. 1976. Waters of the sea: The ocean's characteristics and circulation. Chapter 2 *In* The ecology of the seas. Cushing, D. H. and J. J. Walsh (ed.). W.B. Saunders Co. Philadelphia. 465 p.
- Sun, C-L., S-P. Wang, and S-Z Yeh. 1999. Determination of age and growth of swordfish *Xiphias gladius* L. in the waters of Taiwan using anal fin spines. Working document presented at the Meeting of the Interim Scientific Committee for tuna and tuna-like species in the North Pacific ocean. Jan. 15-23, 1999, Honolulu, HI, USA.
- Suzuki, Z., Y. Warashina and M. Kishida. 1977. The comparison of catches by regular and deep longline gears in the western and central equatorial Pacific. *Bull. Far Seas Res. Lab.* 15: 51-89.
- Turchin, P. 1998. Quantitative analysis of movement. Sinauer Assoc. Sunderland, Mass., USA. 196 p.
- Uchiyama, J.H., and R. S. Shomura. 1974. Maturation and fecundity of swordfish, *Xiphias gladius*, from Hawaiian waters. P. 142-147 *In* Shomura, R.S., and F. Williams (eds.) Proceedings of the 1972 Int. Billfish Symp. Part II, Review of contributed papers. NOAA Tech. Rep. NMFS. SSRF-675.

- Uchiyama, J.H., E.E. DeMartini, and H.A. Williams. 1999. Length-weight interrelationships for sword fish, *Xiphias gladius* L., caught in the central North Pacific. NOAA-TM-NMFS-SWFSC-284. 81 pp.
- Uozumi, Y., K. Yokowa. 1999. Japanese swordfish fisheries in the Pacific Ocean. P. 3-8 *In* Proceedings of the Second International Pacific Swordfish Symposium. DiNardo, G. T. (ed.) NOAA Technical Memorandum NMFS, June 1999. NOAA-TM-NMFS-SWFSC-263. 240 pp.
- Ward, P.J. 1996. Japanese longlining in eastern Australian waters 1962-1990. Bureau of Resource Sciences, Canberra. 250 pp.

11. Tables

Table 1. Principal model components, information type, and data source. Information labels indicate information is known with certainty (A), estimates were obtained from investigations (B), parameters and functions proposed in the absence of reliable estimates (C), parameters and functions based on preliminary studies (D).

Model component	Category				Principal data source
	A	B	C	D	
Growth rate		X			NMFS investigation
Length-at-age		X			NMFS investigation
Weight-at-length		X			NMFS investigation
Maturation rate		X			NMFS investigation
Mating success			X		Ecological theory
Spawning period		x		X	NMFS studies
Egg production		x			Atlantic stock studies
Recruitment pattern		x		X	Literature review
Stock-recruit function			X	X	VPA Atlantic stock
Natural mortality			X	X	Numerical simulations
Swimming rate		x			Tracking studies
Distribution pattern			X		NMFS database records
Movement pattern			X		CPUE trends
Catchability			X	X	CPUE trends
Gear selectivity			X		CPUE trends
Effort distribution	x	x			NMFS database records
Catch composition	x	x	X	X	NMFS database records
Sampling rates			X	X	NMFS database records
Measurement errors			X	X	NMFS investigations

Table 2. Annuli observed versus the possible number of annuli present. The figures are proportions of total number of cross-sections examined by the NMFS ageing staff.

Obs.	1	2	3	4	5	Real 6	7	8	9	10	11	12	13
1	0.96	0.04											
2	0.02	0.97	0.01										
3		0.01	0.98	0.01									
4			0.01	0.98	0.01								
5				0.01	0.98	0.01							
6					0.01	0.98	0.01						
7						0.01	0.97	0.02					
8							0.01	0.97	0.02				
9								0.01	0.97	0.02			
10									0.01	0.97	0.02		
11										0.02	0.96	0.02	
12											0.02	0.96	0.02

Table 3. Boundaries and attributes of regions. The symbols N_, S_, E_ and W_
[bound] refer to Northern, Southern, Eastern, and Western boundaries.
Hyphenated longitudes indicate boundaries at the north and south. Areas
computed as if areas 1 and 10 are triangles and regions 2-9 are trapezoids.

Region	N_bound (Lat.)	S_bound (Lat.)	W_bound (Lon.)	E_bound (Lon.)	
1	46 N	25 N	138-118 E	148 E	
2	46 N	39 N	148 E	170 W	
3	39 N	32 N	148 E	170 W	
4	32 N	25 N	148 E	170 W	
5	25 N	0	118-100 E	170 W	
6	46 N	39 N	170 W	128 W	
7	39 N	32 N	170 W	128 W	
8	32 N	25 N	170 W	128 W	
9	25 N	0	170 W	108-75 W	
10	46 N	25 N	128 W	128-108 W	
Region	N_bound (km)	S_bound (km)	Middle (km)	Height (km)	Area (km ² /1E3)
1	773	3020	1897	2340	3533
2	3209	3600	3405	779	2652
3	3600	3989	3795	779	2956
4	3989	4219	4104	779	3197
5	7166	10018	8592	2782	23903
6	3209	3600	3405	779	2652
7	3600	3989	3795	779	2956
8	3989	4219	4104	779	3197
9	6194	10575	8385	2782	23326
10	232	2015	1124	2340	2358

Table 4. Hypothesized swordfish movement rates ($\text{km}\cdot\text{d}^{-1}$) across boundaries from origin [O] to destination [D]. Hyphens indicate no movement is likely.

[O]	[D]									
	1	2	3	4	5	6	7	8	9	10
1	-	195	65	25	0	-	-	-	-	-
2	0	-	25	-	-	29	-	-	-	-
3	0	25	-	25	-	-	25	-	-	-
4	25	-	25	-	25	-	-	25	-	-
5	175	-	-	25	-	-	-	-	17	-
6	-	21	-	-	-	-	25	-	-	29
7	-	-	25	-	-	25	-	25	-	25
8	-	-	-	25	-	-	25	-	25	25
9	-	-	-	-	34	-	-	25	-	8
10	-	-	-	-	-	21	25	25	42	-

Table 5. Hypothesized dispersal rates ($\%\text{N}\cdot\text{d}^{-1}$) across adjacent boundaries, from region of origin [O] to destination [D]. Hyphens indicate no dispersal.

[O]	[D]									
	1	2	3	4	5	6	7	8	9	10
1	-	0.034	0.011	0.004	0.000	-	-	-	-	-
2	0.000	-	0.032	-	-	0.009	-	-	-	-
3	0.000	0.032	-	0.032	-	-	0.007	-	-	-
4	0.006	-	0.032	-	0.032	-	-	0.006	-	-
5	0.027	-	-	0.005	-	-	-	-	0.002	-
6	-	0.006	-	-	-	-	0.032	-	-	0.009
7	-	-	0.007	-	-	0.032	-	0.032	-	0.007
8	-	-	-	0.006	-	-	0.032	-	0.032	0.006
9	-	-	-	-	0.004	-	-	0.006	-	0.001
10	-	-	-	-	-	0.006	0.007	0.007	0.018	-

Table 6. Summary of test results from the production model analysis. The values in shaded cells represent the 'known' values used to generate the catch-effort series. See text for description of case scenarios, testing conditions, and column labels.

Test	No	Ko	Beta	r	m	q1	q2	MSY	MSY_b	MSY_h	MSY_f
Actual	11038	11038	-	0.5578	2.0000	0.0033	0.0033	1539	5519	0.2789	84.51
1	14376	13683	1.0507	0.4326	2.3977	2.36E-03	-	1480	6842	0.2163	91.77
2	14376	13683	1.0507	0.4326	2.3977	2.36E-03	2.36E-03	1480	6842	0.2163	91.77
3	14732	14129	1.0426	0.4692	2.2033	2.29E-03	2.84E-03	1657	7065	0.2346	102.48
4	9858	9787	1.0072	0.8606	2.0347	3.32E-03	3.86E-03	2106	4894	0.4303	129.76
5	10788	10846	0.9947	0.7636	2.0381	3.00E-03	3.50E-03	2070	5423	0.3818	127.34
6	8403	8602	0.9769	0.8893	2.0472	3.88E-03	4.62E-03	1912	4301	0.4447	114.68
Actual	11038	11038	-	1.0544	2.0000	3.30E-03	3.30E-03	2910	5519	0.5272	159.76
7	8593	7802	1.1013	1.2929	2.0047	4.02E-03	3.38E-03	2522	3901	0.6464	160.89
8	2.9E+08	1.3E+08	2.2819	0.9696	1.9542	1.45E-07	1.35E-07	3.1E+07	6.4E+07	0.4848	3.3E+06
9	922101	406212	2.2700	0.9776	1.9560	4.60E-05	1.35E-07	99278	203106	0.4888	10626.0
10	7190	8723	0.8243	1.1509	1.9979	4.31E-03	3.32E-03	2510	4362	0.5755	133.52
11	7177	8710	0.8240	1.1511	1.9979	4.31E-03	3.32E-03	2506	4355	0.5755	133.67
12	12373	15916	0.7774	0.4717	2.0151	2.67E-03	1.63E-03	1877	7958	0.2358	88.26
13	5430	3688	1.4726	1.7425	1.9995	9.94E-11	5.05E-10	1606	1844	0.8713	8.7E+09

12. Figures

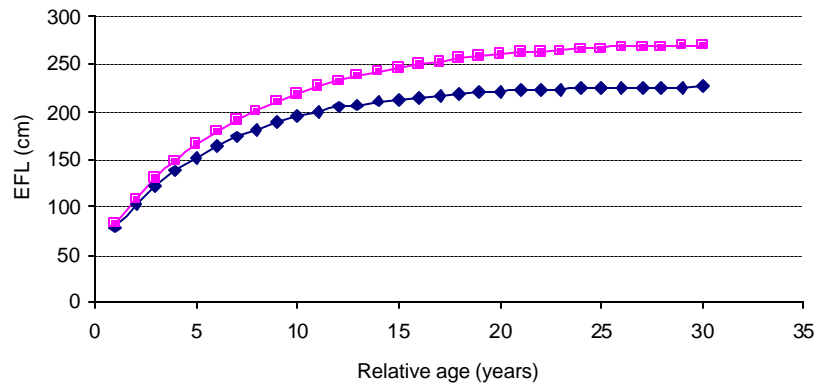


Figure 1. Predicted mean length-age for females (top line) and male swordfish.

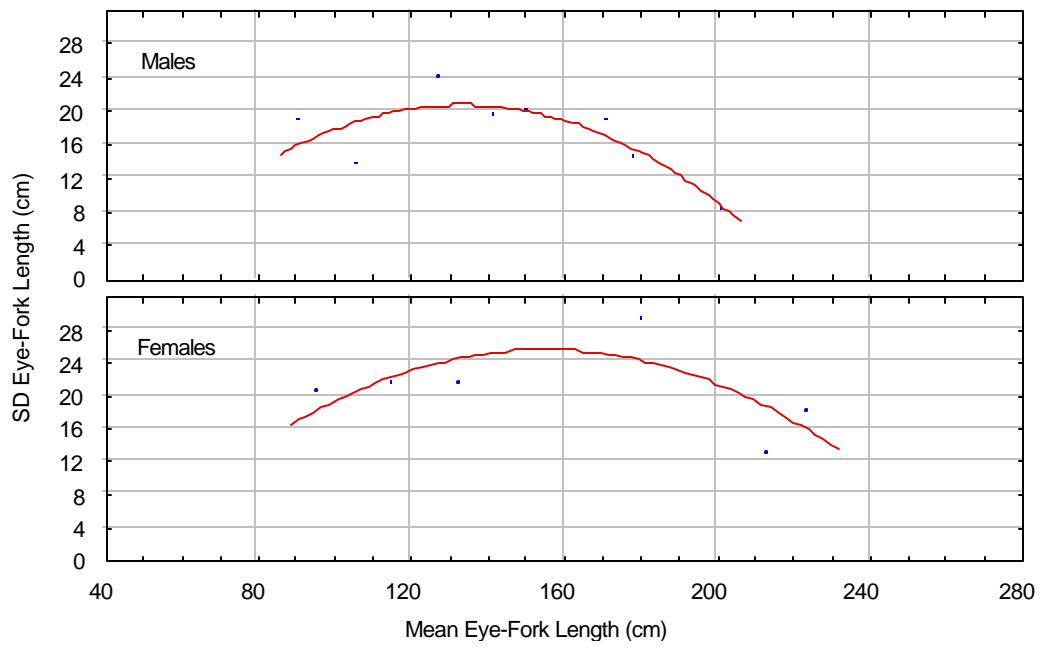


Figure 2. Sample standard deviation (SD) in length-at-age against mean lengths. Solid line indicates trend predicted with quadratic function.

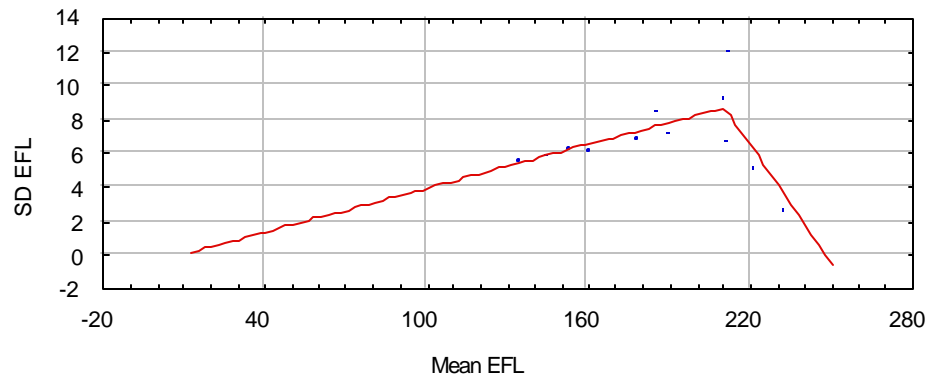


Figure 3. Breakpoint regression of standard deviation in eye-fork length against mean eye-fork length for swordfish (sexes combined) in successive 20-kg weight categories.

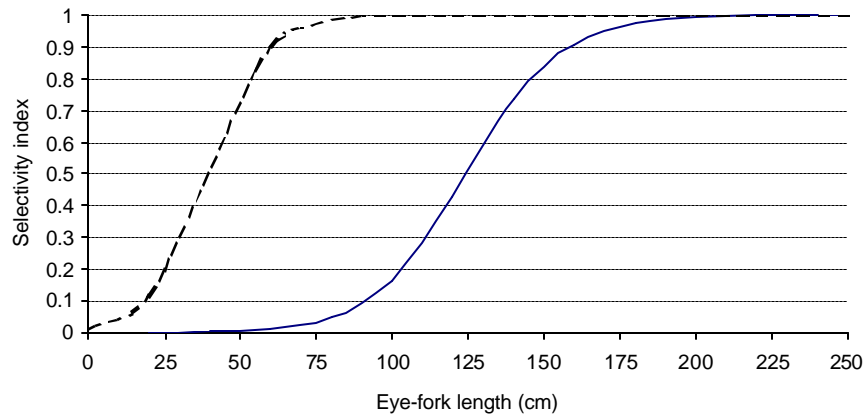


Figure 4. Hypothesized gear selectivity patterns for swordfish harvested in longline fisheries (Type I, broken line) and those harvested by a combination of drift gillnet, harpoon, and recreational fisheries (Type II, solid line).

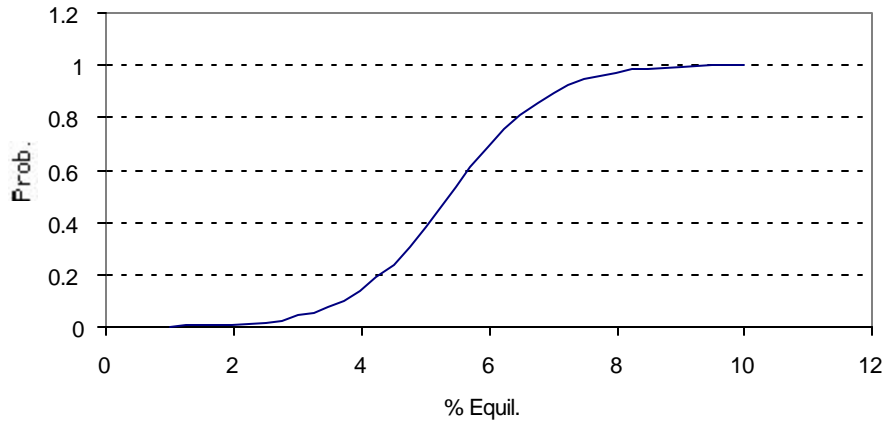


Figure 5. Probability of contacting mates against the relative density of effective spawners.

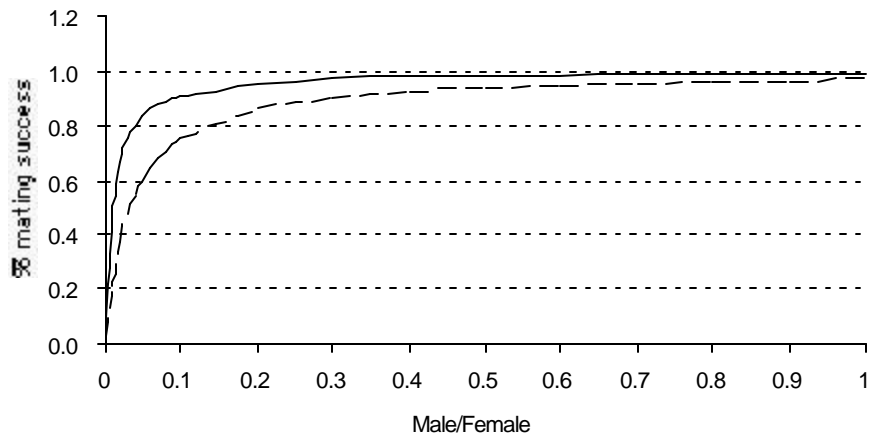


Figure 6. Female mating success against male/female ratio at two levels of relative density of effective spawners (top curve $p > 10\%$; bottom curve $p = 5\%$).

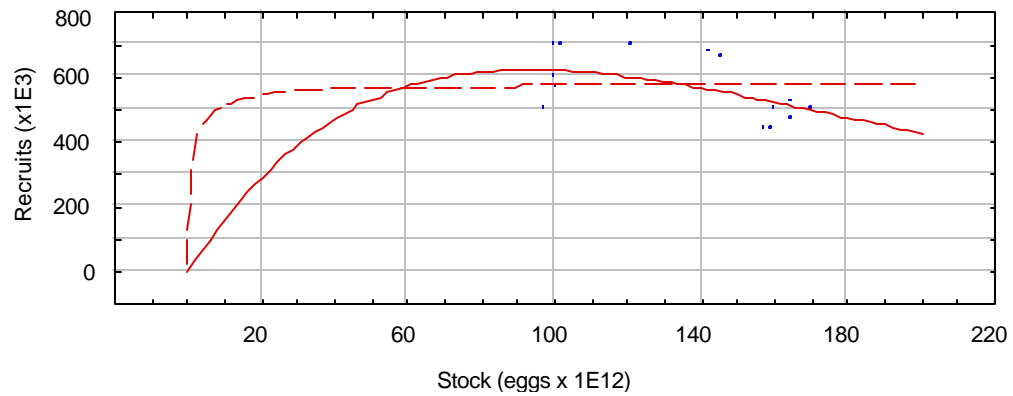


Figure 7. Stock-recruit relations fitted to Atlantic swordfish data resulting from the 1994 base case assessment conducted by ICCAT (see Garcia-Saez 1996). Recruitment levels indicate number of age-1 fish. Predicted recruitment levels represented by solid and dashed lines are for the Ricker (1954) and Beverton-Holt (1957) models respectively.

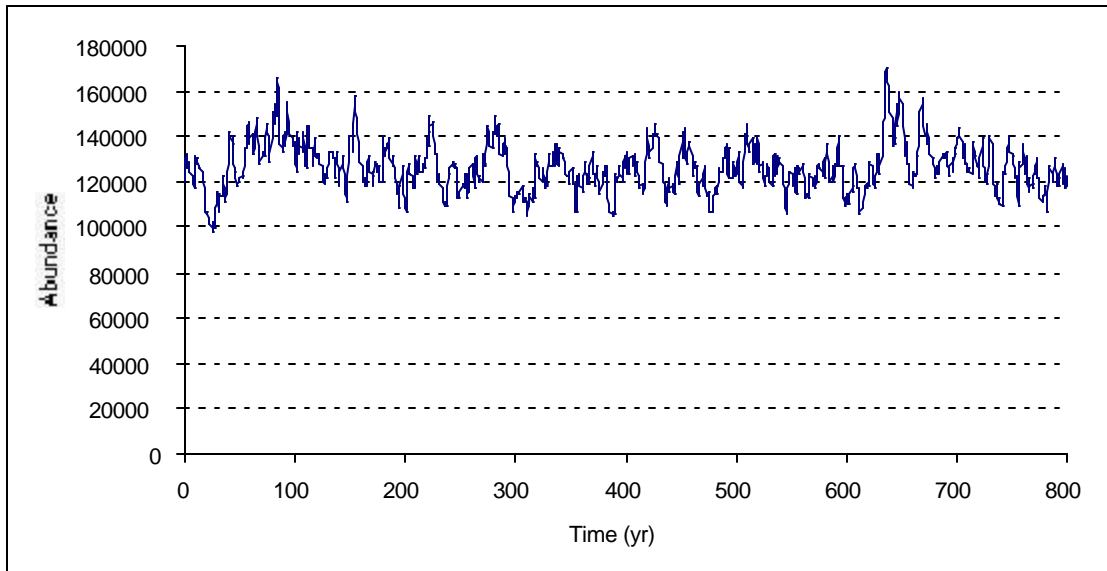


Figure 8. Simulated trends in standing stock biomass over 2,000 years, given $Z=0.2$ and modest levels of stochastic (log-normal) variation in recruitment predicted with a Beverton-Holt (1957) function.

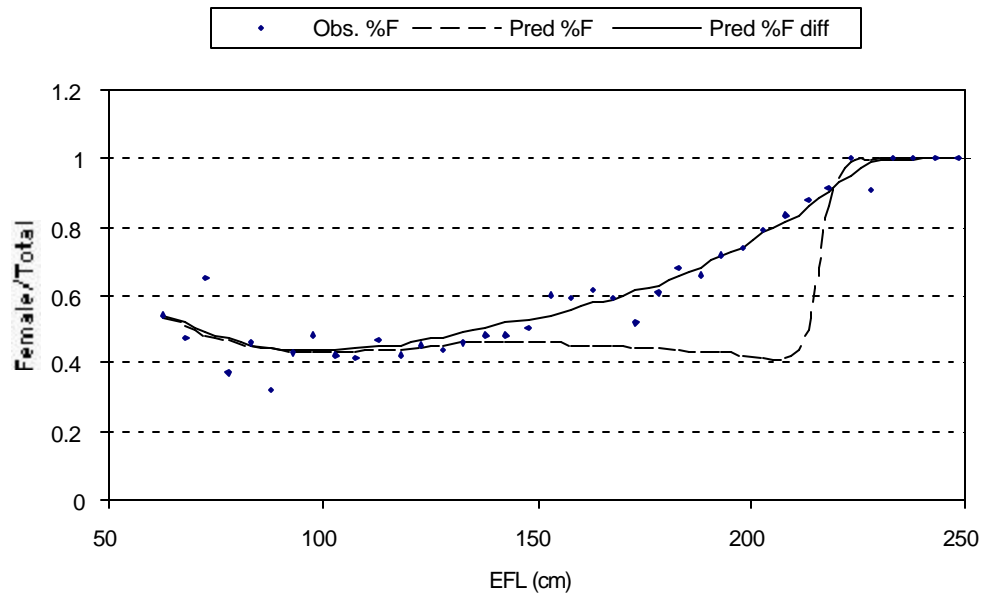


Figure 9. Female contributions in longline catch samples by 5 cm size category. Observed values are represented by dots. Contributions predicted with and without sex-specific natural mortality rates are represented by solid and broken lines respectively.

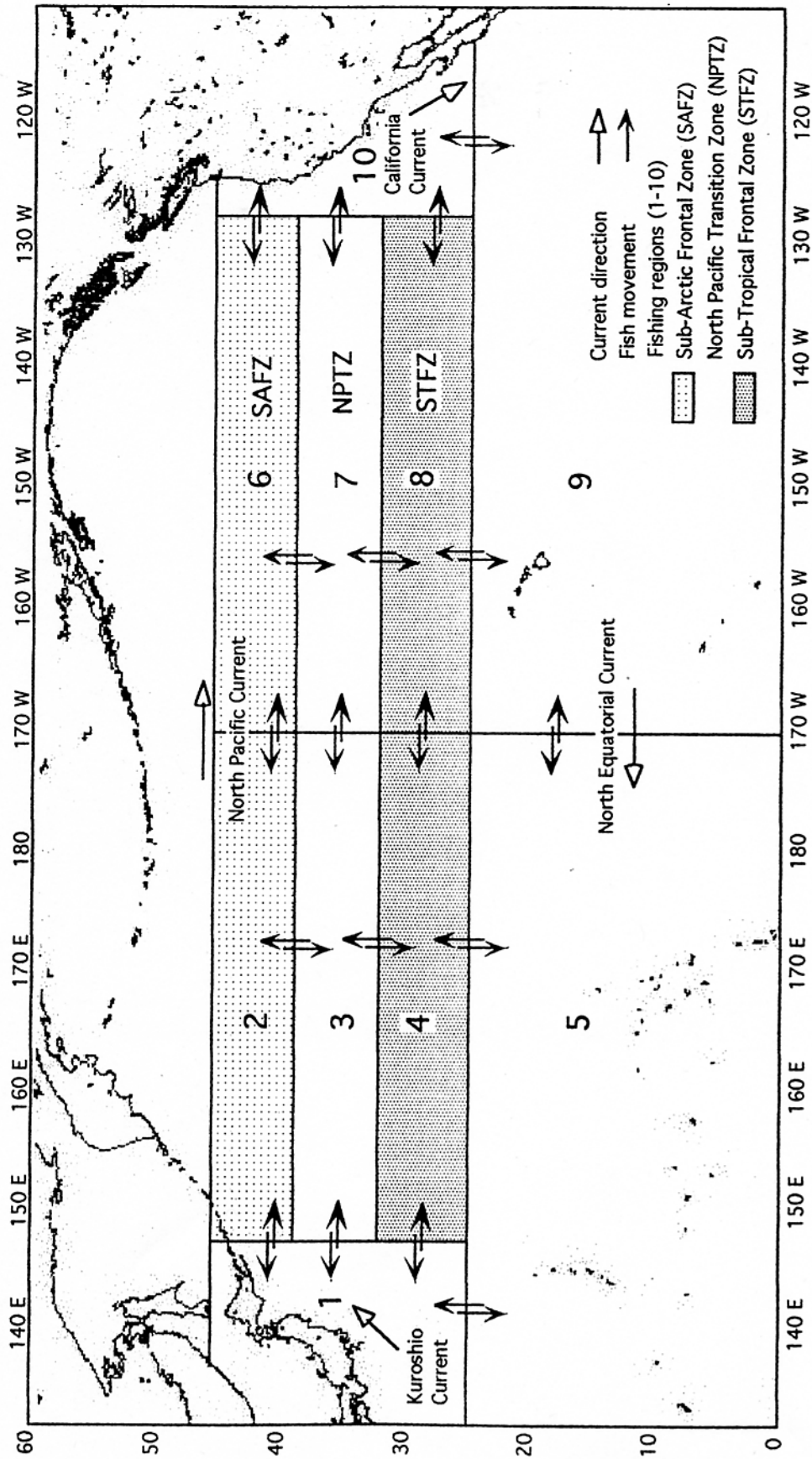


Figure 10. Major features of the North Pacific, used for spatial stratification and movement modeling.

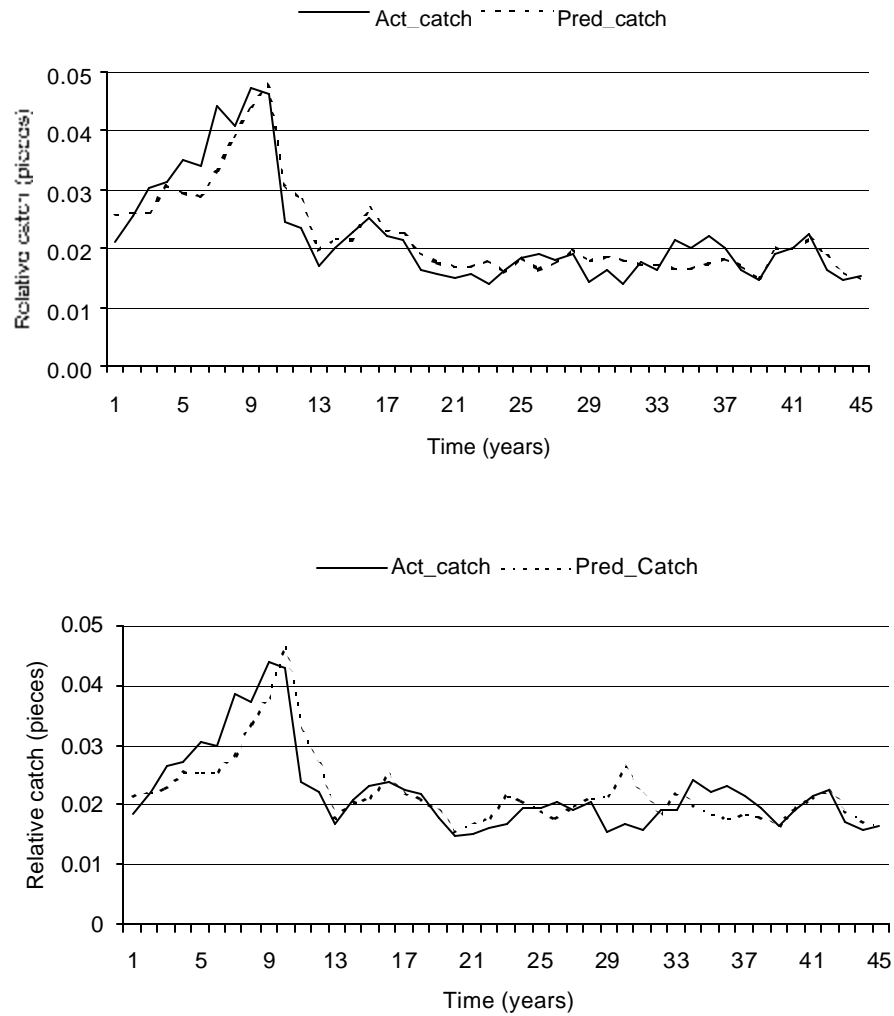


Figure 11. Actual and predicted catch levels based on Japanese and US longline fishing effort only over 1952-1996 (top) and for all fisheries (bottom). Relative catches were obtained by dividing annual catches by the sum of catches over the simulation period. Natural mortality rates for males and females were 0.43 and 0.15 respectively.

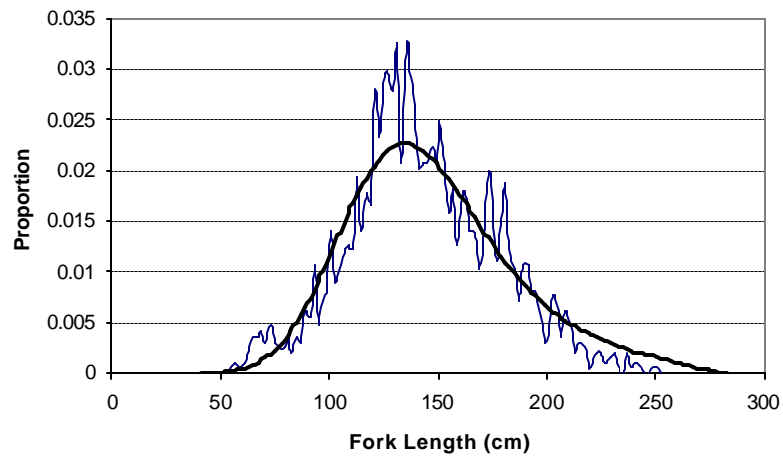


Figure 12. Actual (thin, jagged line) and predicted (bold, smooth line) size frequency distribution of swordfish caught in the Hawaiian longline fishery, based on 1994 sample data.

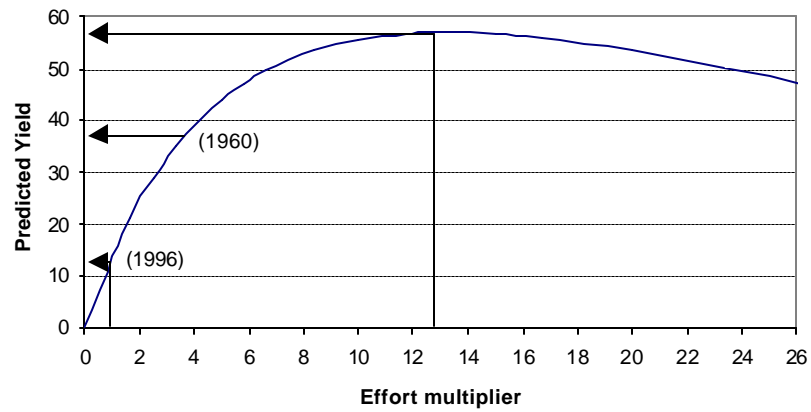
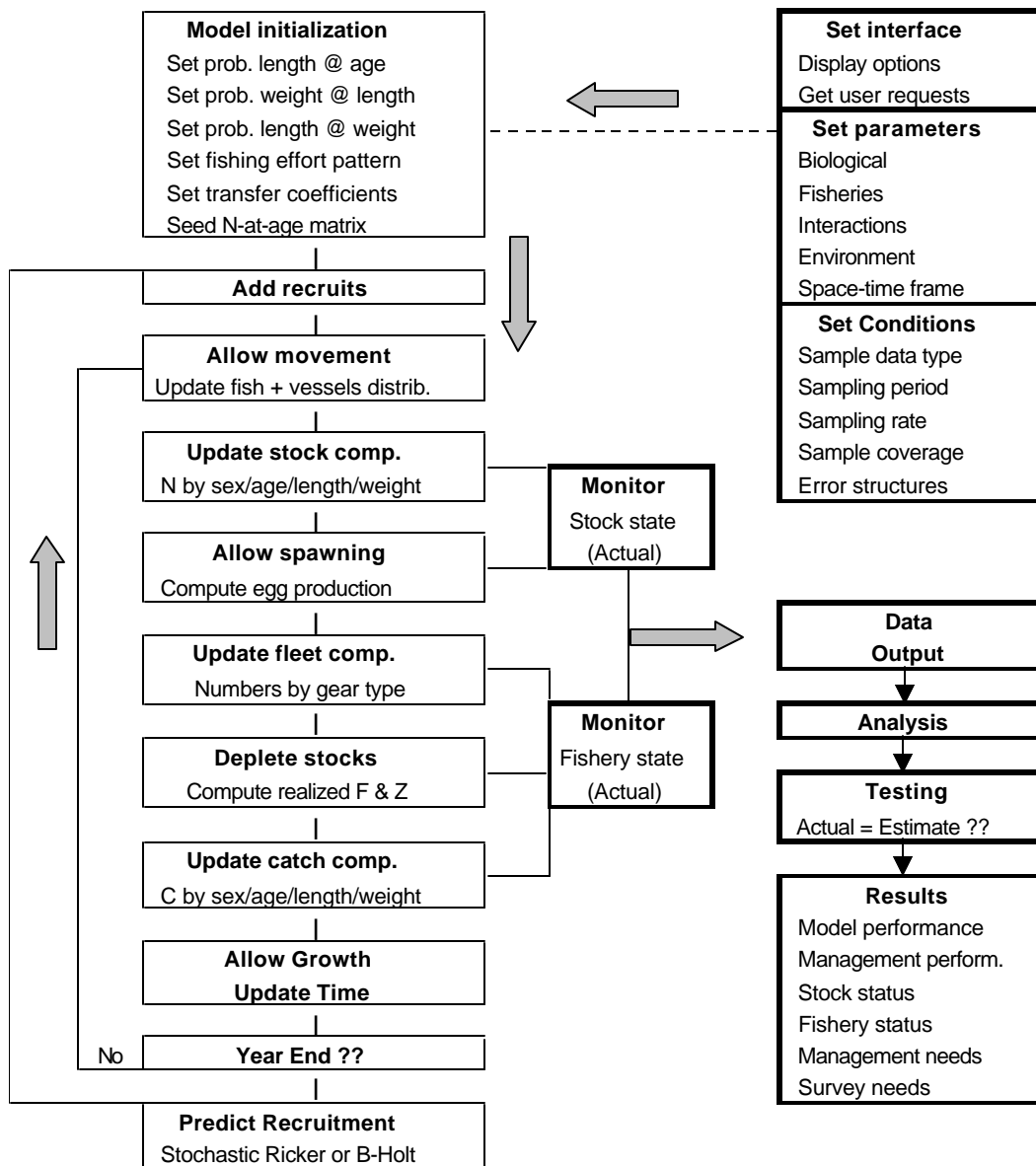


Figure 13. Predicted yield versus total fishing effort. The peak of the curve corresponds to the predicted long-term yield (LTY) and corresponding effort index, relative to the baseline year (1996) and the year of the highest historical catch (1960).

APPENDIX I

PELAGIC FISHERY SIMULATION MODEL STRUCTURE



APPENDIX II

Procedure to compute mating success

The spawning success model is derived from Holling's (1959) disk equation used to describe species interactions. The following notation is used for this section only.

s	= subscript denoting sex (male=0, female=1)
h	= spawning period
g	= searching period
T _h	= total spawning time
T _g	= total search time
T	= total time
X	= total number of mating events
p	= probability of finding a mate during a period
A	= area searched during a period
d _s	= fish density of a given sex, stratum
D	= total fish density in a stratum
η _s	= number of effective spawners of a given sex in a stratum
λ _t	= probability of female mating during a period

Consider a population of one female and several males. A female time budget is first computed using a procedure described by Hilborn and Walters (1992, p. 124). Let T_h = Xh and X = PAd₀T_g, then T_g = X/PAd₀. Setting A to unity, the number of mates a female can spawn with is

$$(1) \quad T = T_h + T_g \equiv \frac{X}{pAd_0} + hX \equiv X \left(\frac{1}{pAd_0} + h \right).$$

$$(2) \quad X = \frac{T}{\frac{1}{pAd_0} + h} \equiv \frac{TpAd_0}{1 + pAhd_0} \equiv \frac{Tp d_0}{1 + p h d_0}.$$

Eq. 2 is a functional relation with the shape and mathematical form of a rectangular hyperbola ($y = \alpha x / \beta + x$) when $x = p d_0 h$ and $\alpha = T/h$. The predicted curve has an asymptote α and equals $\alpha/2$ at $x = \beta$ (i.e. $X = T/2h$ at $p d_0 h = 1$). Dividing X by the asymptote results in a simple equation that predicts a proportion equal to 1.0 when a female attains the maximum number of spawning events possible

$$(3) \quad \frac{X}{X_{\max}} = \frac{\left(\frac{Tp d_0}{1 + p h d_0} \right)}{\frac{T}{h}} = \frac{p h d_0}{1 + p h d_0} .$$

Eq. 3 is a function of spawning time, density, and probability of contact. Substituting male density by the ratio of effective spawners in a stratum gives an index of mating success that is a function of the relative availability of males

$$(4) \quad l = \frac{\frac{h_0}{h_1} p h}{1 + \left(\frac{h_0}{h_1} p h \right)} .$$

At low densities, spawning success should decrease irrespective of the male/female ratios. So the probability of contact is modeled as a logistic function of effective spawners relative to some threshold value consisting of the number of effective spawners at equilibrium

$$(5) \quad t = 100 \frac{h_1 + h_0}{h_0^* + h_1^*} .$$

$$(6) \quad p = \frac{e^{a+bt}}{1 + e^{a+bt}} .$$

Values for a and b can be selected subjectively to make the predicted curve conform to some expectation about its shape. In Figure 5, $a = -7.0$, $b = 1.3$, so the probability of contact is almost 1.0 when the number of effective spawners is =10% of the equilibrium level and declines in a sigmoid fashion to zero below this level. As a result, the probability of finding mates is only compromised at very low levels of abundance irrespective of the sex ratio in the population.

Appendix III

NMFS PACIFIC OCEAN PELAGIC FISHERY SIMULATION PROGRAM [V 8.5]
 EXPECTED VALUES AND PSEUDO-OBSERVATIONS CAN BE GENERATED FOR

{1} Stock size by yr	{2} Stock size by yr/mo
{3} Stock size by yr/age	{4} Stock size by yr/mo/age
{5} Stock size by yr/len	{6} Stock size by yr/mo/len
{7} Stock size by yr/wt	{8} Stock size by yr/mo/wt
{9} Catch size by yr	{10} Catch size by yr/mo
{11} Catch size by year/age	{12} Catch size by yr/mo/age
{13} Catch size by yr/len	{14} Catch size by yr/mo/len
{15} Catch size by yr/wt	{16} Catch size by yr/mo/wt
{17} Mean age stock by yr	{18} Mean age stock by yr/mo
{19} Mean age catch by yr	{20} Mean age catch by yr/mo
{21} Mean length stock by yr	{22} Mean length stock by yr/mo
{23} Mean length catch by yr	{24} Mean length catch by yr/mo
{25} Mean weight stock by yr	{26} Mean weight stock by yr/mo
{27} Mean weight catch by yr	{28} Mean weight catch by yr/mo
{29} Stock biomass by yr	{30} Stock biomass by yr/mo
{31} Spawning biomass by yr	{32} Spawning biomass by yr/mo
{33} Catch biomass by yr	{34} Catch biomass by yr/mo
{35} Recruitment by yr	{36} Realized F-at-age by yr/mo

ACCORDING TO THE FOLLOWING CRITERIA & CONDITIONS

{0-2} Sex required: Males, Females, or Both
 {0-9} Mean catch underreporting rate (1 = 10%)
 {0-1} Catch counting/recording errors (no/yes)
 {0-1} Lengths from weight-length conversions (no/yes)
 {0-1} Ageing errors (no/yes)
 {0-1} Stock-recruit function (Ricker/Bev-Holt)
 {0-4} Baseline annual M (.10, .15, .20, .25, .30)
 {0-1} Differential mortality, male > female (no/yes)
 {0-1} Non-linear C/E vs N (no/yes)
 {0-1} Variation in catchability (no/yes)
 {0-1} Allee effects (no/yes)
 {0-9} Random number sequence
 {0-1} Array bounds checking (no/yes)

ENTER 14 INTEGER (SPACED) FOR OPTIONS NEEDED, OR HIT Q TO QUIT

9 2 0 0 0 0 0 1 1 0 0 0 0 0

Options chosen: 9 2 0 0 0 0 0 1 1 0 0 0 0 0

Results in => Option_9.txt

Setting up matrices and building up population...

Steady state reached at year 30: R = 2000/yr F = 0.0/yr Baseline M = 0.15/yr
 Effect_spawn index = 3399.92 Egg production = 1.15048e+012
 Matching recruit. = 2000 Pre-juv. survival = 1.73841e-009
 S/R scale coef.1 = 2.56625e+010 S/R scale coef.2 = 6.49569

Simulation in progress.....

RECENT TECHNICAL MEMORANDUMS

Copies of this and other NOAA Technical Memorandums are available from the National Technical Information Service, 5285 Port Royal Road, Springfield, VA 22167. Paper copies vary in price. Microfiche copies cost \$9.00. Recent issues of NOAA Technical Memorandums from the NMFS Southwest Fisheries Science Center are listed below:

- NOAA-TM-NMFS-SWFSC-331 Ichthyoplankton and station data for Manta (surface) tows taken on California Cooperative Oceanic Fisheries Investigations Survey Cruises in 1995.
E.M. SANDKNOP, R.L. CHARTER, H.G. MOSER
(May 2002)
- 332 Ichthyoplankton and station data for Manta (surface) tows taken on California Cooperative Oceanic Fisheries Investigations Survey Cruises in 1996.
W. WATSON, R.L. CHARTER, H.G. MOSER
(May 2002)
- 333 Ichthyoplankton and station data for Manta (surface) tows taken on California Cooperative Oceanic Fisheries Investigations Survey Cruises in 1997.
D.A. AMBROSE, R.L. CHARTER, H.G. MOSER
(May 2002)
- 334 Ichthyoplankton and station data for Manta (surface) tows taken on California Cooperative Oceanic Fisheries Investigations Survey Cruises in 1998.
D.A. AMBROSE, R.L. CHARTER, H.G. MOSER
(May 2002)
- 335 Ichthyoplankton and station data for Manta (surface) tows taken on California Cooperative Oceanic Fisheries Investigations Survey Cruises in 1999.
D.A. AMBROSE, R.L. CHARTER, H.G. MOSER
(May 2002)
- 336 Ichthyoplankton and station data for Manta (surface) tows taken on California Cooperative Oceanic Fisheries Investigations Survey Cruises in 2000.
W. WATSON, R.L. CHARTER, H.G. MOSER
(May 2002)
- 337 Ichthyoplankton and station data for surface (Manta) and oblique (Bongo) plankton tows taken during a survey in the eastern tropical Pacific ocean July 30-December 9, 1998.
D.A. AMBROSE, R.L. CHARTER, H.G. MOSER, S.R. CHARTER, and W. WATSON
(June 2002)
- 338 Ichthyoplankton and station data for surface (Manta) and oblique (Bongo) plankton tows taken during a survey in the eastern tropical Pacific ocean July 28-December 9, 1999.
W. WATSON, E.M. SANDKNOP, S.R. CHARTER, D.A. AMBROSE, R.L. CHARTER, and H.G. MOSER
(June 2002)
- 339 Report of ecosystem studies conducted during the 1997 Vaquita abundance survey on the research vessel David Starr Jordan.
V.A. PHILBRICK, P.C. FIEDLER, and S.B. REILLY
(June 2002)
- 340 The Hawaiian Monk Seal in the Northwestern Hawaiian Islands, 2000.
Compiled and edited by: T.C. JOHANOS and J.D. BAKER
(August 2002)